

F-theory fluxes, Chirality and Chern-Simons theories

Thomas W. Grimm¹ and Hirotaka Hayashi²

¹*Max Planck Institute for Physics
Föhringer Ring 6
Munich, 80805, Germany*

²*School of Physics
Korea Institute for Advanced Study
Seoul 130-722, Korea*

grimm at mppmu.mpg.de, hayashi at kias.re.kr

ABSTRACT: We study the charged chiral matter spectrum of four-dimensional F-theory compactifications on elliptically fibered Calabi-Yau fourfolds by using the dual M-theory description. A chiral spectrum can be induced by M-theory four-form flux on the fully resolved Calabi-Yau fourfold. In M-theory this flux yields three-dimensional Chern-Simons couplings in the Coulomb branch of the gauge theory. In the F-theory compactification on an additional circle these couplings are only generated by one-loop corrections with charged fermions running in the loop. This identification allows us to infer the net number of chiral matter fields of the four-dimensional effective theory. The chirality formulas can be evaluated by using the intersection numbers and the cones of effective curves of the resolved fourfolds. We argue that a study of the effective curves also allows to follow the resolution process at each co-dimension. To write simple chirality formulas we suggest to use the effective curves involved in the resolution process to determine the matter surfaces and to connect with the group theory at co-dimension two in the base. We exemplify our methods on examples with $SU(5)$ and $SU(5) \times U(1)$ gauge group.

Contents

1. Introduction	2
2. F-theory chirality and three-dimensional Chern-Simons theories	5
2.1 Resolving Calabi-Yau fourfolds	5
2.2 G_4 -form fluxes and their F-theory interpretation	8
2.3 Four-dimensional chirality formula from three-dimensional loops	10
3. Strategy to derive chirality formulas on resolved fourfolds	14
3.1 The relative Kähler and Mori cone	14
3.2 Mori cone, singularity resolution, and connection with group theory	15
3.3 Matter surfaces and the chiral index	20
4. Examples	22
4.1 A Calabi-Yau hypersurface with $SU(5)$ gauge group	22
4.2 A $U(1)$ -restricted hypersurface with $SU(5) \times U(1)$ gauge group	31
5. Conclusions	40
A. Six-dimensional matter via five-dimensional loops	42
B. Mori cone of hypersurfaces in toric varieties	45
C. Resolution from Tate form	47

1. Introduction

In the last years there has been vast progress in understanding four-dimensional F-theory compactifications on elliptically fibered Calabi-Yau fourfolds. These compactifications can admit non-Abelian gauge groups which arise from stacks of 7-branes. Geometrically this corresponds to a degeneration of the elliptic fiber over divisors in the base wrapped by the seven-branes [1, 2]. At the intersection of two such divisors matter fields are localized. The presence of a 7-brane flux can lift part of the matter spectrum such that a net number of chiral fields remain in the $\mathcal{N} = 1$ low energy effective supergravity theory. The aim of this paper is to determine formulas for the net number of such fields depended on the global geometric data of resolved Calabi-Yau fourfolds and the specification of four-form fluxes. To justify the proposed chirality formulas we will exploit the duality between M-theory and F-theory, including one-loop corrections to the Chern-Simons terms in the effective theories obtained from M-theory.

A first approach in the derivation of a chirality formula for the charged matter fields along the intersection of two 7-branes was to use the local data of the geometry and gauge bundle [3, 4, 5]. The required data included the classes of the matter curves and the local two-form flux components on the 7-branes. For these consideration the input mainly came from two directions. In [3, 5] a spectral cover construction, more familiar from the heterotic string [6], has been used. In contrast, the formulas in [4] intensively use the local 7-brane gauge theory and more closely resemble the Type IIB analogs known from a weak coupling picture with D-branes. Despite these successes it is in general hard to obtain a global picture and develop the tools to study more complicated 7-brane configurations. In addition to the construction of compact Calabi-Yau fourfolds a complete global treatment has also to capture the flux data, which requires a deep understanding of the local singular geometry near the 7-branes and its global embedding. An analysis of the global geometry is particularly crucial when additional $U(1)$ symmetries are present [7, 8]. Extensions of the spectral cover techniques to global constructions have been proposed in [9, 10, 11, 12, 13]. In particular, in [10, 11, 13] consistency checks have been given to argue for the applicability of the spectral cover techniques to specific compact settings. In the present work we will take a different route, since we will specify the flux data directly on the resolved Calabi-Yau fourfolds with no reference to a spectral cover construction.

Let us summarize our general strategy to derive chirality formulas in F-theory. Firstly, note that to study F-theory compactifications one inevitably has to address the fact that non-Abelian gauge groups arise from singular Calabi-Yau geometries X_4 for which the geometrical data determining the spectrum and couplings cannot be determined directly. However, a natural way to deal with the singularities is to perform a resolution of the singularities and work with the fully resolved Calabi-Yau fourfold \tilde{X}_4 . Such resolutions can be performed using toric methods as in [14, 15, 10, 11, 16, 17, 18, 19], or stepwise as recently shown in [20, 13]. The physics induced by the resolution process can be addressed in the M-theory description of F-theory [1, 2]. M-theory compactification on an resolved elliptically fibered Calabi-Yau fourfold yields a specific three-dimensional effective theory

with a couplings which can arise from a four-dimensional $\mathcal{N} = 1$ supergravity compactified on a circle [21]. For the resolved Calabi-Yau fourfolds the theory will be in the Coulomb branch of the three-dimensional gauge theory.

In the M-theory picture of F-theory the 7-brane fluxes correspond to four-form fluxes G_4 of the field-strength of M-theory three-form potential. Not all G_4 fluxes will lift to a four-dimensional F-theory compactification. Crucially one has to impose that the allowed fluxes preserve four-dimensional Poincaré invariance in the F-theory limit [22]. Further restriction are imposed by demanding the existence of an unbroken four-dimensional gauge theory. It was argued in [13] that there are G_4 fluxes that satisfy these conditions, and reproduce the four-dimensional chirality formulas known from the spectral cover construction of an $SU(5)$ model. The allowed G_4 fluxes crucially involve the wedges of two-forms Poincaré-dual to the exceptional resolution divisors. In this work we will give a physical interpretation of this fact.

To link the G_4 flux with the four-dimensional chirality it is crucial to point out that the M-theory reduction on a Calabi-Yau fourfold with G_4 flux induces terms in the three-dimensional gauge theory which are not obtained by a classical circle reduction of a general four-dimensional gauge theory. This can be inferred from the explicit reduction of [23, 21]. In fact, the M-theory reduction will induce Chern-Simons terms for the $U(1)$ gauge-fields in the Coulomb branch. We note that in the reduction of the four-dimensional theory such terms must arise from one-loop corrections with charged fermions running in the loop. This links the charged matter spectrum of the four-dimensional theory with the G_4 -flux corrections of the M-theory reduction. We will show that this provides us with an interpretation how the chiral matter spectrum can be determined from the flux data.

If the flux indeed encodes the net number of chiral fermions on the intersection curves of two 7-branes, the chiral index has to be of the form $\chi(\mathbf{R}) = \int_{S_{\mathbf{R}}} G_4$, as already anticipated in [3, 5], and studied recently in [24, 13, 18]. Here \mathbf{R} is the representation of the four-dimensional gauge group in which the fermions transform. The intersection curve of the two 7-brane in the base of \tilde{X}_4 will be called matter curve $\Sigma_{\mathbf{R}}$ if matter fields in the representation \mathbf{R} are located along this curve. The difficulty in evaluating the expression for $\chi(\mathbf{R})$ is to give a global and universal definition of the surface $S_{\mathbf{R}}$. Using heterotic/F-theory duality one expects that $S_{\mathbf{R}}$ is obtained by fibering the resolution \mathbb{P}^1 's over the matter curve. In fact, in the M-theory picture the charged matter fields arise from M2-branes wrapping the \mathbb{P}^1 -fibers of the resolved geometry. The group theory matches this geometric interpretation since the resolution \mathbb{P}^1 's over the matter curves can be associated to the weights of the representation \mathbf{R} [25, 26]. These states are massive on the resolved space \tilde{X}_4 and become massless in the singular F-theory limit.

To construct the matter surfaces for a given resolved Calabi-Yau fourfold we propose to exploit the data encoded by the cone of effective curves, i.e. the Mori cone. It will be crucial to select a subcone of the full Mori cone, the relative Mori cone, consisting of curves in \tilde{X}_4 which shrink when going to the singular space X_4 . This cone will be completed into the extended relative Mori cone by including other effective curves in the elliptic fiber,

which intersect the exceptional resolution divisors. In simple cases this simply amounts to including the pinched elliptic fiber over the 7-brane. We will argue that the intersection of these curves with the exceptional divisors allows us to identify a pairing between generators of the extended relative Mori cone and weights of the four-dimensional gauge group. The exceptional divisors correspond to the simple roots of the gauge group. The identification of roots and weights with the geometric data has been proposed for local Calabi-Yau threefolds in [25, 26, 13]. Note that a detailed analysis of which weights correspond to the effective curves in the extended relative Mori cone also allows us to stepwise reconstruct the resolution process along the co-dimension two and three singularity loci in the base of X_4 . In this process, we make two assumptions. One is that the representation which can appear along the co-dimension two singularity loci are the same as the one of the matter fields localized along the curve. The second is that the degeneration of weights at the co-dimension three singularity points obeys the algebra G_p when the singularity is enhanced to a type G_p . These assumptions are exploited already in [27, 3, 4, 28] and have been studied for compact settings in [13, 18]. With these assumptions and the extended relative Mori cone at hand, we can generally determine the resolution process along the singularity loci.

In this work we also include that case where additional geometrically massless $U(1)$ gauge fields are in the four-dimensional spectrum of the F-theory compactification. The methods to determine the resolution structure using the extended Mori cone naturally generalize to this situations, and one is able to explicitly construct the matter surfaces $S_{\mathbf{R}}$ also if distinguishing $U(1)$ -charges of the representation \mathbf{R} are present. However, one can generalize the Ansatz for the G_4 flux if one permits a gauging of the four-dimensional $U(1)$ -symmetries. Such extra fluxes render the $U(1)$ massive, but allow to keep its global selection rules. An explicit example how such extra $U(1)$'s can be consistently induced in a Calabi-Yau fourfold compactification was given in [8], and termed $U(1)$ -restricted Tate model. The construction of fluxes in this model have been recently given in [24, 18]. In reference [24] a direct link to the chirality formulas for D7-branes and O7-planes was established. For $SU(5)$ models and their extensions it was shown in [18] that the chirality formula can be evaluated using the ambient fivefold geometry in which the Calabi-Yau fourfold is embedded. These techniques also allowed to reduce the G_4 fluxes, using the ambient fivefold, to a two-form flux on the base \mathcal{B} , and reproducing the correct group theoretical factors as required for a valid chirality formula. In our formalism this detour is not required, and the $U(1)$ case appears as natural part of a more general construction.

To illustrate the derivation of the net chiralities we will consider two explicit examples of hypersurfaces in toric ambient spaces. The gauge theory will be $SU(5)$ and $SU(5) \times U(1)$ and we perform an explicit resolution of all co-dimension singularities as in [10, 11, 17, 8, 18] by modifying the toric ambient space. We compute the net chiralities induced by a general G_4 flux compatible with four-dimensional Poincaré invariance and the preservation of the $SU(5)$ gauge symmetry in both cases. Our results are compared to the spectral cover and split spectral cover constructions [29, 9, 10], and we find match of the chirality formulas for matter being localized near the $SU(5)$ -brane as expected.

2. F-theory chirality and three-dimensional Chern-Simons theories

In this section we give a derivation of the F-theory chirality formulas by using one-loop corrections in a dual three-dimensional Chern-Simons theory. More precisely, we will exploit the description of F-theory via M-theory to show that a four-dimensional chiral spectrum can be induced by a special class of G_4 -form fluxes on a resolved Calabi-Yau fourfold \tilde{X}_4 . This will lead to a derivation of formulas of the form

$$\chi(\mathbf{R}) = n_{\mathbf{R}} - n_{\mathbf{R}^*} = \int_{S_{\mathbf{R}}} G_4, \quad (2.1)$$

where $S_{\mathbf{R}}$ is a four-cycle in \tilde{X}_4 . Here we have denoted by $\chi(\mathbf{R})$ the chiral index of $n_{\mathbf{R}}$ matter fields in the representation \mathbf{R} minus $n_{\mathbf{R}^*}$ matter fields in the representation \mathbf{R}^* .

In order to interpret chirality formulas involving G_4 we first have to summarize the properties of a fully resolved Calabi-Yau fourfold \tilde{X}_4 in section 2.1. In the compactification of M-theory on \tilde{X}_4 one can allow for G_4 fluxes in the reduction. We describe the M-theory and F-theory constraints on these fluxes in section 2.2. It is argued in section 2.3 that a certain class of M-theory fluxes induces Chern-Simons couplings in the three-dimensional effective theory. The matching these M-theory couplings with one-loop corrections of an F-theory setup compactified on a circle leads to chirality formulas of the form (2.1).

For completeness we establish a similar analysis for F-theory compactifications to six dimensions on elliptically fibered Calabi-Yau threefolds in appendix A. We include explicit formulas for the $SU(N)$ case. A more elaborated discussion of this duality including gravity can be found in [30].

2.1 Resolving Calabi-Yau fourfolds

Let us consider an elliptically fibered Calabi-Yau fourfold X_4 with fibers which can be singular over each complex co-dimension of the base \mathcal{B} . We further demand that these singularities can be consistently resolved while still preserving the Calabi-Yau condition. Numerous Calabi-Yau three- and fourfold examples with various gauge groups have been constructed in refs. [14, 15, 10, 11, 16, 17, 18] as hypersurfaces and complete intersections inside a toric ambient space. One can show that the singularities are resolved by adding new blow-up divisors to the ambient toric space. This can be done systematically as argued in [14, 15]. Note that only on the resolved Calabi-Yau manifolds one can straightforwardly compute the topological data of the geometry. These are required to determine the spectrum and couplings of the F-theory compactification [21]. The toric resolutions are equivalent, at least at co-dimension one and two relevant here, to the small resolutions performed for an $SU(5)$ gauge group in [20, 13].¹

For simplicity let us focus on geometries with a single gauge group G over a divisor $S_{\mathbf{b}} = S \cdot \mathcal{B}$ in the base \mathcal{B} of the Calabi-Yau manifold. Here the dot denotes the intersection of the divisors S and \mathcal{B} . The resolved Calabi-Yau fourfold will be named \tilde{X}_4 in the following.

¹We like to thank D. Klevers for explicitly checking this equivalence.

We denote the set of inequivalent exceptional resolution divisors and the Poincaré-dual two-forms by

$$D_i, \omega_i, \quad i = 1, \dots, \text{rank}(G). \quad (2.2)$$

In addition we have divisors and Poincaré-dual two-forms

$$D_\alpha, \omega_\alpha, \quad \alpha = 1, \dots, h^{1,1}(\mathcal{B}), \quad (2.3)$$

The divisors D_α are obtained from divisors in the base \mathcal{B} as pre-image of the projection $\pi : X_4 \rightarrow \mathcal{B}$ if there is no gauge group located along divisors $D_\alpha \cdot \mathcal{B}$. However, after the blow-up one has to modify the divisor S in X_4 which hosts the gauge group G . One introduces the redefinition

$$S = \hat{S} + \sum_i a_i D_i, \quad (2.4)$$

where a_i are the Dynkin labels of the group G . Note that this modification has to be taken into account when introducing a basis D_α on \tilde{X}_4 . In such a basis one has the expansion

$$S = C^\alpha D_\alpha. \quad (2.5)$$

The simplest situation is that S is one of the divisors D_α . Finally, if the elliptic fibration only has a single section, we introduce the two-form ω_0 Poincaré-dual to the base \mathcal{B} itself.

There are various generalizations to this setup. In particular, the geometry can induce additional $U(1)$ factors due to its fibration structure or additional singularities over curves in \mathcal{B} . The number of extra $U(1)$'s is counted by

$$n_{U(1)} = h^{1,1}(\tilde{X}_4) - h^{1,1}(\mathcal{B}) - \text{rank}(G). \quad (2.6)$$

A particular example with an extra $U(1)$ is the $U(1)$ -restricted Tate model discussed in [8]. The geometry is in this case restricted such that the discriminant locus develops an additional singularity over a curve, which after resolution induces a new two-form ω_X . In general, each extra $U(1)$ comes with a new element $\tilde{\omega}_m$ of $H^{1,1}(\tilde{X}_4)$, and can be represented by a divisor \tilde{D}_m . Note that the two-forms $\tilde{\omega}_m$ have intersection properties similar to the ω_i introduced above. Hence, it will be useful to introduce the combined notation

$$D_\Lambda = (D_i, \tilde{D}_m), \quad \omega_\Lambda = (\omega_i, \tilde{\omega}_m), \quad \Lambda = 1, \dots, \text{rank}(G) + n_{U(1)}. \quad (2.7)$$

As we will recall below, the D_Λ have to have special intersection properties such that the corresponding gauge-fields are well-defined in four dimensions. This will allow to select an appropriate basis for D_Λ .

It is important to stress that in F-theory the resolution \tilde{X}_4 is not physical. In fact, the F-theory compactification to four space-time dimensions has to be carried out on the singular space X_4 where the full non-Abelian gauge symmetry is present. However, the space \tilde{X}_4 can be used in the dual M-theory compactification. Recall that it is natural to describe F-theory via M-theory [1, 2]. Starting with M-theory this interpretation requires to perform a T-duality along one of the one-cycles of the elliptic fiber of X_4 after going to

Type IIA by shrinking the size of the elliptic fiber. Note that in the dual Type IIB setup the shrinking of the elliptic fiber corresponds to a decompactification to four space-time dimensions. The compactification on the resolved space \tilde{X}_4 is thus only possible in the M-theory picture, before shrinking the sizes of the elliptic fiber and the resolution divisors. In such a generic point in the Kähler moduli space of \tilde{X}_4 , one is in the Coulomb branch of the three-dimensional gauge theory obtained by the M-theory compactification. The gauge group is

$$U(1)^{\text{rank}(G)} \times U(1)^{n_{U(1)}} . \quad (2.8)$$

The $U(1)$ gauge bosons arise from the expansion of the M-theory three-form C_3 into the two-form ω_Λ introduced in (2.7) as

$$C_3 = A^\Lambda \wedge \omega_\Lambda , \quad \Lambda = 1, \dots, \text{rank}(G) + n_{U(1)} . \quad (2.9)$$

Only in the limit in which the exceptional divisors D_i shrink to the holomorphic surface S one recovers the non-Abelian gauge symmetry G present in the four-dimensional F-theory compactification.

Having a fully resolved Calabi-Yau fourfolds \tilde{X}_4 , one can compute the complete set of intersection numbers, and other topological data such as Chern classes. Let us here summarize the structure of intersection numbers. For a hypersurface or complete intersection in a toric ambient space they can be determined explicitly by inducing the intersection structure of the ambient space. The intersections depend on the ‘triangulation’ as we will make more precise for the examples below. This implies that there will be various topological phases associated to an ambient space and its Calabi-Yau manifold [31]. We introduce the quadruple intersections as

$$\mathcal{K}_{ABCD} = \int_{\tilde{X}_4} \omega_A \wedge \omega_B \wedge \omega_C \wedge \omega_D , \quad (2.10)$$

where $\omega_A = (\omega_0, \omega_\alpha, \omega_\Lambda)$. For resolved elliptically fibered Calabi-Yau fourfolds one has several vanishing conditions for the intersection numbers. Firstly, recall that for four divisors inherited from the base \mathcal{B} one obviously has

$$\mathcal{K}_{\alpha\beta\gamma\delta} = 0 . \quad (2.11)$$

More subtle are the vanishing intersections involving the blow-up divisors D_Λ . The following vanishing conditions hold:

$$\mathcal{K}_{\Lambda\alpha\beta\gamma} = 0 , \quad \mathcal{K}_{0\Lambda AB} = 0 , \quad (2.12)$$

where A, B run over all possible indices as in (2.10). To justify this recall that ω_Λ parameterizes the $U(1)$ ’s in (2.8) through the expansion (2.9). However, these are three-dimensional gauge fields in an M-theory compactification on \tilde{X}_4 . In order that they lift to four-dimensional gauge fields the two conditions (2.12) have to be satisfied [21]. In fact, for the explicit resolutions performed below, this condition is satisfied for an appropriate basis D_Λ . Clearly, the conditions (2.12) are consequences of the geometry of resolved elliptic fibrations.

Let us now turn to the non-vanishing intersections. For a single gauge group G with resolution divisors D_i one finds

$$\mathcal{K}_{ij\alpha\beta} = -C_{ij} C^\gamma \mathcal{K}_{0\alpha\beta\gamma} , \quad (2.13)$$

where C^α has been introduced in (2.5). C_{ij} is the Cartan matrix of the algebra associated to the gauge group G . Note that the conditions (2.11), (2.12) and (2.13) are independent of the phase, or triangulation, of the resolution part of \tilde{X}_4 .² Of crucial importance for the chirality formulas will be the intersection numbers:

$$\mathcal{K}_{\alpha\Lambda\Sigma\Gamma} , \quad \mathcal{K}_{\Lambda\Sigma\Gamma\Delta} , \quad (2.14)$$

with three or four exceptional divisors D_Λ introduced in (2.7). These crucially depend on the phase as we will see below. Let us note that the basis used for the computation of these intersection numbers is adapted to the structure of the elliptic fibration. A basis adapted to the Kähler cone, measuring positive volumes in the Calabi-Yau manifold, will be discussed in section 3.1.

2.2 G_4 -form fluxes and their F-theory interpretation

In this section we introduce the G_4 fluxes on the resolved Calabi-Yau fourfold \tilde{X}_4 . The G_4 fluxes have to be considered in the M-theory picture of F-theory and correspond to a non-trivial field strength of the M-theory three-form C_3 . Together with the results of section 2.3, this will allow us to find the set of fluxes which induce a net chiral matter spectrum along the intersection curves of the 7-branes in the F-theory limit.

Let us first summarize some of the key properties of G_4 . The flux is an element of the fourth cohomology group $H^4(\tilde{X}_4, \mathbb{R})$. It can be split into a horizontal and vertical part $H_V^4 \oplus H_H^4$, where H_V^4 is obtained by wedging two forms of $H^2(\tilde{X}_4, \mathbb{R})$, and H_H^4 are the four-forms which can be reached by a complex structure variation of the holomorphic $(4, 0)$ -form on \tilde{X}_4 . In the following we will be concerned with fluxes in $H_V^4(\tilde{X}_4, \mathbb{R})$, which can be written as

$$G_4 = m^{AB} \omega_A \wedge \omega_B , \quad (2.15)$$

where ω_A is the basis introduced in section 2.1. There are constraints on G_4 , both from an M-theory and an F-theory perspective. Firstly, M-theory anomalies demand that G_4 is properly quantized [32]

$$G_4 + \frac{1}{2} c_2(\tilde{X}_4) \in H_V^4(\tilde{X}_4, \mathbb{Z}) . \quad (2.16)$$

This condition is crucial for fluxes in H_V^4 since the second Chern class $c_2(\tilde{X}_4)$ is in this component of H^4 . The quantization condition has recently been discussed in [33, 18] for specific gauge groups or specific geometries. However, let us stress that in general it is a hard question to determine a minimal integral basis of $H_V^4(\tilde{X}_4, \mathbb{Z})$.³

²In might be necessary to reorder the divisors D_i to keep the same form of (2.13).

³In particular, even if one shows that a component of $c_2(\tilde{X}_4)$ can be written as $a\omega \wedge \tilde{\omega}$ for the effective $\omega, \tilde{\omega}$, the integrality of the coefficient a does not imply that $\frac{a}{2}\omega \wedge \tilde{\omega}$ is non-integral. A fancy way to determine an integral basis is by using mirror symmetry [34].

Let us now turn to the constraints on G_4 imposed in the F-theory perspective. In order that the M-theory fluxes G_4 actually lift to F-theory fluxes without breaking four-dimensional Poincaré invariance and keeping the whole group G unbroken, we have to enforce that various components of G_4 vanish. In order to do that we define⁴

$$\Theta_{AB} = \int_{\tilde{X}_4} G_4 \wedge \omega_A \wedge \omega_B . \quad (2.17)$$

The fluxes relevant for our F-theory compactifications have to satisfy

$$\begin{aligned} \Theta_{0\alpha} &= 0 , & \Theta_{\alpha\beta} &= 0 , \\ \Theta_{i\alpha} &= 0 . \end{aligned} \quad (2.18)$$

Let us comment on these various constraints. The first two constraints are conditions on the existence of a Poincaré invariant four-dimensional theory. $\Theta_{0\alpha}$ correspond in the M-theory to F-theory limit to fluxes along the circle when performing the 4d/3d compactification as discussed in detail in [36]. The fluxes $\Theta_{\alpha\beta}$ are mapped to non-geometric fluxes in F-theory and make the existence of a four-dimensional effective theory questionable. Note that the fluxes $\Theta_{\Lambda 0}, \Theta_{00}$ are automatically vanishing due to (2.12), and the fact that $\Theta_{00} = \Theta_{0\alpha} K^\alpha$ with a vector K^α parameterizing the first Chern class of \mathcal{B} . The second line in (2.18) are conditions on an unbroken gauge group G . $\Theta_{i\alpha}$ is readily interpreted in the M-theory to F-theory limit. These fluxes have a four-dimensional interpretation and would induce gaugings of the axionic parts of the complexified Kähler moduli. This yields a breaking of the group G , which we demand to be unbroken in our considerations. In summary, we find that the only non-vanishing components of Θ_{AB} are given by

$$\Theta_{\Lambda\Sigma} = \int_{\tilde{X}_4} G_4 \wedge \omega_\Lambda \wedge \omega_\Sigma , \quad \Theta_{\alpha m} = \int_{\tilde{X}_4} G_4 \wedge \omega_\alpha \wedge \tilde{\omega}_m . \quad (2.19)$$

where ω_i, ω_j are the two-forms Poincaré dual to the resolution divisors, and $\tilde{\omega}_m$ are the forms parameterizing extra $U(1)$'s as introduced in (2.7).

Let us make some further comments on the significance of $\Theta_{\alpha m}$. In (2.18) we have demanded $\Theta_{\alpha i} = 0$ to prevent breaking the gauge group by a gauging involving the Cartan generators only. For the extra $U(1)$'s such a gauging is precisely induced by $\Theta_{\alpha m}$, and we did not restrict to the case where it has to vanish. In fact the gauge invariant derivatives are

$$DT_\alpha = dT_\alpha + i\Theta_{\alpha m} A^m . \quad (2.20)$$

Here T_α are the complexified Kähler volumes of the divisors in the base \mathcal{B} . The precise definition of T_α as well as the lift of (2.20) from M-theory to F-theory can be found in [21, 35]. The presence of the gauging (2.20) implies that the $U(1)$ can become massive by a Higgs effect. In fact, A^m can ‘eat’ the imaginary part of T_α and gain a new degree of freedom as required for a massive $U(1)$. Due to supersymmetry such a gauging induces also a D-term, which gives a mass to the real part of T_α . This massive scalar appropriately combines with A^m into a massive four-dimensional $\mathcal{N} = 1$ vector multiplet.

⁴Note that we changed the definition of Θ_{AB} compared with [35, 36]. The chosen definition will be convenient in the match with the four-dimensional result.

2.3 Four-dimensional chirality formula from three-dimensional loops

Recall that in order to find a well-defined framework to deal with fluxes in F-theory we have used the fact that F-theory can be obtained as a limit of M-theory. In this limit four-dimensional F-theory compactifications on a singular Calabi–Yau fourfold X_4 are obtained from an M-theory compactification on the resolved fourfold \tilde{X}_4 in the limit of shrinking elliptic fiber and shrinking exceptional divisors. The two setups are best compared in three dimensions where the M-theory compactification on \tilde{X}_4 has to match a circle compactification of the four-dimensional F-theory effective action [21]. In the following we will argue that the M-theory compactification with G_4 induces additional Chern-Simons terms which are not induced by a classical Kaluza-Klein reduction of a four-dimensional $\mathcal{N} = 1$ gauge theory on a circle. The match is achieved only after including one-loop corrections with charged matter fermions running in the loop.

Let us start by recalling some crucial facts about M-theory on a Calabi-Yau fourfold \tilde{X}_4 [23, 21]. As in (2.8) the three-dimensional gauge group is broken to $U(1)^{\text{rk}G} \times U(1)^{n_{U(1)}}$ when performing the reduction on a resolved Calabi–Yau fourfold. Hence, the M-theory effective theory will be in the Coulomb branch in three-dimensional gauge theory. Note that the three-dimensional $\mathcal{N} = 2$ vector multiplets contain as bosonic fields

$$(\xi^\Lambda, A^\Lambda), \quad \Lambda = 1, \dots, \text{rk}G + n_{U(1)}, \quad (2.21)$$

where the ξ^Λ are real scalars. The A^Λ are the $U(1)$ gauge fields from the dimensional reduction of the M-theory three-form as in (2.9), while the ξ^Λ parameterize the size of the blow-ups in the M-theory compactification on \tilde{X}_4 . The ξ^Λ arise in the expansion of the normalized Kähler form $\tilde{J} = J \cdot \mathcal{V}^{-1}$, where \mathcal{V} is the overall volume of \tilde{X}_4 . Explicitly, one expands

$$\tilde{J} = \xi^\Lambda \omega_\Lambda + L^\alpha \omega_\alpha + R\omega_0, \quad (2.22)$$

where $\omega_\alpha, \omega_\Lambda$ are the two-forms introduced in (2.3), (2.7), and ω_0 is the Poincaré dual to the base \mathcal{B} .

The key observation is that the inclusion of G_4 fluxes in the M-theory reduction induces a Chern-Simons term in the three-dimensional effective action. In particular, for the vector multiplets (2.21) one finds a Chern-Simons term

$$S_{\text{CS}}^{(3)} = \frac{1}{4} \int_{\mathbb{M}^{2,1}} \Theta_{\Lambda\Sigma} A^\Lambda \wedge F^\Sigma \quad (2.23)$$

where $\Theta_{\Lambda\Sigma}$ is given in terms of the G_4 flux as in (2.19), and F^Λ is the field strength of A^Λ . Due to the $\mathcal{N} = 2$ supersymmetry of the three-dimensional theory $\Theta_{\Lambda\Sigma}$ has to be constant, which is consistent with (2.19).

We now turn to the F-theory picture, and consider a general $\mathcal{N} = 1$ gauge theory compactified to three dimensions on a circle. The four-dimensional theory is identified with the low energy effective theory obtained by reducing F-theory on a Calabi-Yau fourfold X_4 . In the four-dimensional theory the charged fermions χ^s appear with a kinetic term [37]

$$K_{r\bar{s}} \bar{\chi}^s \mathcal{D} \chi^r, \quad (2.24)$$

where \mathcal{D}_μ is the covariant derivative under the four-dimensional gauge group, and $K_{r\bar{s}}$ is the Kähler metric for the matter multiplets. After compactification on S^1 , the terms (2.24) will induce a coupling of the fermions to the S^1 -component of the four-dimensional vectors. These components are identified with the ξ^Λ if one move to the Coulomb branch of the gauge theory [21], where the vector fields also span the Abelian group (2.8). The resulting three-dimensional coupling is a mass term for the χ^r with mass parameter ξ^Λ . We aim to compare the three-dimensional theories of M-theory and F-theory after Kaluza-Klein reduction. In a general framework of three-dimensional Abelian gauge theories, the quantum-corrected coupling of the Chen-Simons term $\frac{1}{2} \int (k_{\Lambda\Sigma})_{\text{eff}} A^\Lambda \wedge F^\Sigma$ can be written as [38]

$$(k_{\Lambda\Sigma})_{\text{eff}} = (k_{\Lambda\Sigma})_{\text{class}} + \frac{1}{2} \sum_f (q_f)_\Lambda (q_f)_\Sigma \text{sign} \left(\sum_{\Gamma=1}^{\text{rk}G} (q_f)_\Gamma \xi^\Gamma + \tilde{m}_f \right), \quad (2.25)$$

where the second term arises from a one-loop diagram with charged fermions running in the loop. Hence, f runs through all the charged fermions, $(q_f)_\Lambda$ is a $U(1)_\Lambda$ charge and \tilde{m}_f is the classical mass of the fermions. Since the three-dimensional theories we consider originate from the dimensional reduction of four-dimensional $\mathcal{N} = 1$ supersymmetric gauge theories, the classical Chern-Simons term with these indices is absent [21, 36], i.e. $(k_{\Lambda\Sigma})_{\text{class}} = 0$. Furthermore, since the fermions are massless in the F-theory limit $\xi^\Lambda \rightarrow 0$ one also has to set $\tilde{m}_f = 0$. Therefore, comparing the Chern-Simons couplings (2.23) of the M-theory reduction with the general one-loop expression (2.25) we find the relation⁵

$$\Theta_{\Lambda\Sigma} = \frac{1}{2} \sum_f (q_f)_\Lambda (q_f)_\Sigma \text{sign} \left(\sum_{\Gamma=1}^{\text{rk}G} (q_f)_\Gamma \xi^\Gamma \right). \quad (2.26)$$

This expression gives the link between the G_4 fluxes on \tilde{X}_4 and the number of fermions running in the loop if the charges $(q_f)_\Gamma$, and the sign-factors are given. We will now determine these data using the geometric M-theory setting.

To see how the right-hand side of (2.26) can be written by the geometric data we have to recall how the fermionic states arise in M-theory. Recall that in F-theory the matter fields arise from strings stretching between two 7-branes intersecting over a matter curve $\Sigma_{\mathbf{R}}$. Here we will indicate by \mathbf{R} the representation of the four-dimensional gauge group in which the matter fields localized on this curve transform. In the M-theory picture these string states correspond to M2-branes. More precisely, in the resolved phase \tilde{X}_4 the matter multiplets arise from M2-branes wrapped on the resolution \mathbb{P}^1 's fibered over the matter surface [2]. Crucially, one can establish a map between the weights of the representation \mathbf{R} and the resolution \mathbb{P}^1 fibered over the matter curves $\Sigma_{\mathbf{R}}$ [25, 26, 13]. Therefore we will denote the resolution curves associated to a weight \mathbf{w} by $\mathcal{C}_{\mathbf{w}}$. We will discuss this identification in much more detail in section 3. Using this map one can give a geometric formula for the $U(1)_\Lambda$ charge of an M2-brane wrapping on a curve $\mathcal{C}_{\mathbf{w}}$. The charge $(q_f)_\Lambda$

⁵In the match of M-theory with F-theory a factor 1/2 has to be taken into account. This has been discussed in [35, 36] for the gauge coupling function $f_M = 1/2 f_F$, f_F is the three-dimensional gauge coupling obtained after circle reduction.

for the fields is given by

$$(q_f)_\Lambda = q_\Lambda^{\mathbf{w}} = \int_{\mathcal{C}_{\mathbf{w}}} \omega_\Lambda , \quad (2.27)$$

where we have used that $U(1)$ charge of a fermion does only depend on the weight to which it corresponds. The real scalar ξ^i is obtained from the expansion of the Kähler form as in (2.22). Hence, we can rewrite the sign part of (2.26) as

$$\text{sign} \sum_{k=1}^{\text{rk}G} (q_f)_k \xi^k = \text{sign} \int_{\mathcal{C}_{\mathbf{w}}} \tilde{J} \equiv \text{sign}(\mathbf{w}) , \quad (2.28)$$

for a matter field in a weight \mathbf{w} . Here we have used the abbreviation $\text{sign}(\mathbf{w})$ to indicate when a curve is positive or negative, i.e. we introduce the notation

$$\begin{aligned} \mathbf{w} > 0 & \quad \Leftrightarrow \quad \int_{\mathcal{C}_{\mathbf{w}}} \tilde{J} > 0 , \\ \mathbf{w} < 0 & \quad \Leftrightarrow \quad \int_{\mathcal{C}_{\mathbf{w}}} \tilde{J} < 0 . \end{aligned} \quad (2.29)$$

Motivated by the appearance of this sign-factor in (2.26) we will in section 3 introduce in detail the notion of the relative Mori cone. Roughly speaking, the curves in the relative Mori cone are precisely the resolution curves $\mathcal{C}_{\mathbf{w}}$ for which the sign (2.28) is positive. Therefore, providing the techniques to determine the relative Mori cone of a compact Calabi–Yau fourfolds will determine the signs in (2.26).

Let us denote by $n_{\mathbf{r}}$ the number of fermions in the effective three-dimensional theory transforming in a representation \mathbf{r} . Using (2.27) and (2.28) we can rewrite (2.26) as

$$\Theta_{\Lambda\Sigma} = \frac{1}{2} \sum_{\mathbf{r}} n_{\mathbf{r}} \sum_{\mathbf{w} \in W(\mathbf{r})} q_\Lambda^{\mathbf{w}} q_\Sigma^{\mathbf{w}} \text{sign}(\mathbf{w}) , \quad (2.30)$$

where the sum runs over all representations for which $n_{\mathbf{r}}$ fermions appear in the spectrum. From the expression (2.30), one can see that vector-like pairs drop off from the contribution to the Chern-Simons term. If there is a vector-like pair, we always have a pair of weight \mathbf{w} and $-\mathbf{w}$ and their $U(1)$ charges are opposite $q_\Lambda^{-\mathbf{w}} = -q_\Lambda^{\mathbf{w}}$. Then, the contribution from the vector-like pair is

$$\begin{aligned} q_\Lambda^{\mathbf{w}} q_\Sigma^{\mathbf{w}} \text{sign}(\mathbf{w}) + (q_\Lambda^{-\mathbf{w}})(q_\Sigma^{-\mathbf{w}}) \text{sign}(-\mathbf{w}) = \\ q_\Lambda^{\mathbf{w}} q_\Sigma^{\mathbf{w}} \text{sign}(\mathbf{w}) + (-q_\Lambda^{\mathbf{w}})(-q_\Sigma^{\mathbf{w}}) (-\text{sign}(\mathbf{w})) = 0 \end{aligned} \quad (2.31)$$

Therefore, only the chiral indices $\chi(\mathbf{R}) = n_{\mathbf{R}} - n_{\mathbf{R}^*}$ with some numerical factors appear in the right-hand side of (2.30). Clearly, for a given setup one can simply compute the $q_\Lambda^{\mathbf{w}}$ and determine the signs (2.28). This allows to read off $\chi(\mathbf{R})$. Formally, one can write this as

$$\chi(\mathbf{R}) = t_{\mathbf{R}}^{\Lambda\Sigma} \Theta_{\Lambda\Sigma} , \quad (2.32)$$

where $t_{\mathbf{R}}^{\Lambda\Sigma}$ is a matrix associated to the representation \mathbf{R} . In fact, $t_{\mathbf{R}}^{\Lambda\Sigma}$ determines the matter surface $S_{\mathbf{R}}$ appearing in (2.1). In the next section we will present a formalism to

compute $t_{\mathbf{R}}^{\Lambda\Sigma}$ explicitly for a given Calabi-Yau geometry. Let us stress that in the evaluation of (2.30) one uses the three-dimensional fermion spectrum. However, due to the fact that this three-dimensional is obtained as a S^1 compactification of a four-dimensional theory arising from an F-theory compactification, the zero mode spectrum in the three dimensional theories should match that in the four-dimensional theories. In other words, (2.1) equally determines the chirality in F-theory compactifications on the Calabi-Yau fourfold X_4 . One could suspect that there are other modes running in the loop which arise from the Kaluza-Klein tower in the circle compactification. It will be shown in [30] that such modes generate other Chern-Simons couplings but do not contribute in (2.30).

In summary, we need the following data in order to evaluate (2.30) and to determine the chiral index

- A detailed identification of the weights \mathbf{w} with the resolution curves $\mathcal{C}_{\mathbf{w}}$ for a given resolved compact Calabi-Yau fourfold.
- The information about of the sign the Kähler form \tilde{J} integrated over the curves $\mathcal{C}_{\mathbf{w}}$.

Both of these data will be induced in detail in section 3, and evaluated for specific examples in section 4.

To end this section, let us point out that there is an elegant way to encode the match (2.26) by a single auxiliary function \mathcal{T} . One defines \mathcal{T} such that its second derivative with respect to ξ^Λ will generate (2.26). Hence, one has

$$\Theta_{\Lambda\Sigma} = 2 \partial_{\xi^\Lambda} \partial_{\xi^\Sigma} \mathcal{T} . \quad (2.33)$$

From the M-theory perspective a natural definition of \mathcal{T} is

$$\mathcal{T} = \frac{1}{4} \int_{\tilde{X}_4} \tilde{J} \wedge \tilde{J} \wedge G , \quad (2.34)$$

which indeed satisfies (2.33). Let us isolate the part \mathcal{T}^c of \mathcal{T} which encodes the data about the fermionic spectrum running in the loop by defining $\mathcal{T}^c = \frac{1}{2} \xi^\Lambda \xi^\Sigma \partial_{\xi^\Lambda} \partial_{\xi^\Sigma} \mathcal{T}$. Then the condition (2.30) translates into

$$\mathcal{T}^c = \frac{1}{8} \sum_{\mathbf{r}} n_{\mathbf{r}} \sum_{\mathbf{w} \in W(\mathbf{r})} \int_{\mathcal{C}_{\mathbf{w}}} \tilde{J} \Big| \int_{\mathcal{C}_{\mathbf{w}}} \tilde{J} \Big| . \quad (2.35)$$

Note that the real function \mathcal{T} as defined in (2.34) is well-known in the M-theory and F-theory reductions [23, 21, 36]. It encodes not only data about the spectrum, as argued here, but also encodes the three-dimensional scalar potential. In fact, after performing the F-theory limit also the four-dimensional D-terms can be read off from this real function [21]. For example, in the complete expansion of (2.34) also the components $\Theta_{m\alpha}$ appearing in the $U(1)$ -gaugings (2.20) are included and generate the corresponding D-terms.

3. Strategy to derive chirality formulas on resolved fourfolds

In this section we will describe our strategy to explicitly evaluate the formula (2.1) to determine the four-dimensional chiral spectrum induced by non-trivial G_4 flux. The section is divided into several parts which stepwise introduce the geometrical tools to perform the computations. A particular focus will be on the determination of the matter surfaces using the Mori cone generators of the resolved Calabi-Yau fourfold. In outlining the tools we will also explain how details of the resolution process at co-dimension two and three in the base \mathcal{B} can be inferred from the compact geometry using the Mori cone. The discussion of this section will be kept rather general. Examples for which these computations can be carried out explicitly are postponed to section 4.

3.1 The relative Kähler and Mori cone

We have seen in the previous section 2.3 that the evaluation of the one-loop corrections (2.30) requires a detailed knowledge of the positivity of the resolution curve classes. In the following we want to formalize this further. We therefore endow the space of divisors of the resolved fourfolds \tilde{X}_4 with a cone structure by singling out positive Kähler forms. This will allow us to define the relative Kähler cone and relative Mori cone.

Recall that the Kähler cone is spanned by Kähler forms J satisfying the positivity conditions $\int_{\Sigma^k} J^k > 0$, where Σ^k are k -dimensional holomorphic submanifolds of \tilde{X}_4 . The Kähler cone can be spanned by a basis of two-forms or, equivalently, a basis of divisors. The cone dual to the Kähler cone is known as the Mori cone. It is spanned by a basis of effective curves combined with positive coefficients. In the following we want to introduce the *relative Kähler and Mori cones*, which parameterize fields which are driven to a special limit when blowing down the resolutions. Note that the exceptional divisors D_i correspond to the simple roots of G . Since the weights are elements of the dual space to the simple roots, the weights correspond to holomorphic curves $\Sigma_{\mathcal{I}}$ inside the Mori cone, such that

$$D_i \Rightarrow \text{roots} , \quad \Sigma_{\mathcal{I}} \Rightarrow \text{weights} . \quad (3.1)$$

The intersections $D_i \cdot \Sigma_{\mathcal{I}}$ corresponds to the natural dual pairing of weights and roots. We will discuss the precise identification of a given curve with a weight in the next subsection. In the following we want to first give the definitions of the relative cones.

In the shrinking limit of the exceptional divisors D_{Λ} , there are holomorphic curves Σ which are contained in D_{Λ} and map to points in X_4 . We will call the space of all such shrinking curves the relative Mori cone:

$$M(\tilde{X}_4/X_4) = \{\Sigma \mid \Sigma \text{ effective curve mapping to a point in } X_4\}. \quad (3.2)$$

In the M-theory interpretation of the F-theory compactification the charged matter fields arise from M2-branes wrapping on the holomorphic curves Σ as discussed in section 2.3. We have seen in (2.30) that the evaluation of the chirality requires a knowledge about the

positivity of the curves. Later on we will also argue that the relative Mori cone plays a crucial role to identify the resolution process of higher co-dimension singularities.

The dual cone to the relative Mori cone is called the relative Kähler cone $K(\tilde{X}_4/X_4)$. Hence, the relative Kähler cone can be defined as

$$K(\tilde{X}_4/X_4) = \{D = \sum s_\Lambda D_\Lambda \mid D \cdot \Sigma > 0 \text{ for all } \Sigma \in M(\tilde{X}_4/X_4)\}. \quad (3.3)$$

Note that the relative Kähler cone for the Cartan generators of G realized on a singular Calabi-Yau threefold was already introduced in [25]. In this case the negative relative Kähler cone is identified with the sub-wedge of the Weyl chamber of G in five dimensional gauge theories.

Let us introduce a natural extension of the relative Mori cone. We will add additional generators to $M(\tilde{X}_4/X_4)$ which are effective curves in the elliptic fiber, i.e. the Mori cone elements, and intersect the generators of the relative Kähler cone. In simple cases this amounts to including the pinched elliptic fiber over the 7-brane. We will call the resulting cone $\widehat{M}(\tilde{X}_4/X_4)$ the *extended relative Mori cone*. Clearly, we can similarly introduce the *extended relative Kähler cone* $\widehat{K}(\tilde{X}_4/X_4)$ dual to $\widehat{M}(\tilde{X}_4/X_4)$. The cone $\widehat{K}(\tilde{X}_4/X_4)$ will contain one more generator $D_0 = \hat{S}$ which corresponds to the extended node of the Dynkin diagram of G . This generator allows to extend (2.13) to

$$\mathcal{K}_{IJ\alpha\beta} = -C_{IJ} C^\gamma \mathcal{K}_{0\alpha\beta\gamma}, \quad (3.4)$$

where $I = (0, i)$ and C_{IJ} is the extended Cartan matrix.

3.2 Mori cone, singularity resolution, and connection with group theory

Having determined the relative Mori and Kähler cone, we now want to make contact with the group theory of the seven-brane gauge theory with gauge group G . Our key point will be the precise association of some weights of a representation of the gauge group with the elements of the relative Mori cone.

3.2.1 General discussion

We start more general and introduce the charge vectors $\ell_{\mathcal{I},A}$ given by intersecting curves $\Sigma_{\mathcal{I}}$ in the Mori cone with divisors D_A in \tilde{X}_4 as

$$\ell_{\mathcal{I},A} = \int_{\Sigma_{\mathcal{I}}} \omega_A = \Sigma_{\mathcal{I}} \cdot D_A. \quad (3.5)$$

We will determine the $\ell_{\mathcal{I},A}$ for specific examples in section 4. Let us make here some general comments, denoting henceforth by $\ell_{\mathcal{I}}$ the vector with entries (3.5). For Calabi-Yau fourfold examples which are realized as hypersurfaces or complete intersections in a toric ambient space one determines the vectors $\ell_{\mathcal{I}}$ in two steps [39, 40, 41]. Firstly, one uses the set of toric divisors D_A of the ambient space and derives the $\ell_{\mathcal{I}}$ using the Mori cone generators of the ambient space. Since the ambient space can admit many triangulations,

i.e. topological phases connected by flop transitions, one obtains for a given geometry several sets of vectors $\ell_{\mathcal{I}}^{(I)}, \ell_{\mathcal{I}}^{(II)}, \ell_{\mathcal{I}}^{(III)}, \dots$, each set associated to a phase. Restricted to the Calabi-Yau manifold \tilde{X}_4 it can happen that different triangulations of the ambient space are connected by flops of curves which are not in \tilde{X}_4 . This implies that several sets of the ambient space ℓ -vectors have to be combined to describe the ℓ -vectors of the Calabi-Yau manifold \tilde{X}_4 .⁶ Clearly, it will be our task to determine these vectors $\ell_{\mathcal{I}}$ for \tilde{X}_4 itself in section 4. For completeness a brief account of the general procedure to determine the ℓ -vectors for a Calabi-Yau hypersurface is given in appendix B.

Let us now make contact with the gauge theory on the 7-branes. We recall that we are working with the resolved fourfold \tilde{X}_4 and hence are on the Coulomb branch in the M-theory compactification to three dimensions. The geometrically massless gauge fields are then parameterizing the Abelian group (2.8), $U(1)^{\text{rank}(G)} \times U(1)^{n_{U(1)}}$. In connection with this gauge group it will be crucial to analyze the ℓ -vectors associated to $U(1)$ -charges for the divisors D_{Λ} . These are given by

$$\ell_{\mathcal{I},\Lambda} = \Sigma_{\mathcal{I}} \cdot D_{\Lambda} , \quad (3.6)$$

where $D_{\Lambda} = (D_i, \tilde{D}_m)$ as in (2.7). In particular, for the Cartan $U(1)$'s in G one has the Cartan charges $\ell_{\mathcal{I},i} = \Sigma_{\mathcal{I}} \cdot D_i$, where D_i are the resolution divisors corresponding to the Cartan generators of G . One realizes that a curve $\Sigma_{\mathcal{I}}$ will be in the *relative* Mori cone if it has negative intersection with one of the D_{Λ} :

$$\ell_{\mathcal{I},\Lambda} < 0 \quad \Rightarrow \quad \Sigma_{\mathcal{I}} \in M(\tilde{X}_4/X_4) . \quad (3.7)$$

In fact, if the curve $\Sigma_{\mathcal{I}}$ has the negative intersection with D_{Λ} , $\Sigma_{\mathcal{I}}$ is contained in D_{Λ} and shrinks to a point in X_4 . Note that if a curve $\Sigma_{\mathcal{I}}$ is in the base \mathcal{B} itself, the intersection with the D_{Λ} vanishes due to the intersection structure (2.12). This is consistent with the fact that such curves have no $U(1)$ -charges under the group (2.8), and are not in the relative Mori cone.

By computing the $U(1)$ -charges of a curve $\Sigma_{\mathcal{I}}$ with respect to the D_{Λ} , one can next determine a weight which reproduces the same $U(1)$ charges, and associate the weight to the curve $\Sigma_{\mathcal{I}}$ or the ℓ -vector $\ell_{\mathcal{I}}$. This leads to the identification

$$\ell_{\mathcal{I}} \cong \text{weight of a representation of } G . \quad (3.8)$$

Using this method one can associate a weight of G to each generator of the relative Mori cone. This allows us to determine which weights \mathbf{w} correspond to the effective curves and which weights do not. Since we know the weights which correspond to the generators of the relative Mori cone, other weights which correspond to effective curves should be realized by a linear combination of the weights in the relative Mori cone with positive integer coefficients. Applying this process, we determine the complete correspondence

⁶By abuse of notation we have used the same symbols and indices for the ℓ -vectors of the ambient space and the Calabi-Yau manifold \tilde{X}_4 . Let us stress that even the number of ℓ -vectors can differ for the two geometries.

between the weights and the effective curves. Consistent with (2.29) we use the following simplifying notation

$$\begin{aligned} \mathbf{w} > 0 &\Leftrightarrow \mathbf{w} \text{ corresponds to an effective curve} \\ \mathbf{w} < 0 &\Leftrightarrow \mathbf{w} \text{ does not correspond to an effective curve .} \end{aligned} \tag{3.9}$$

We argue in the following that details of the resolution process are contained in this information.

Before turning to the resolution process, let us briefly comment on how one can also represent the roots as curves. In fact, due to the intersection numbers (2.13), we can always introduce a curve $\mathcal{C}_{-\alpha_i}$ associated to the negative of a simple root α_i by the triple intersection of three divisors

$$\mathcal{C}_{-\alpha_i} = D_i \cdot \tilde{D} \cdot \mathcal{D}, \tag{3.10}$$

where $\tilde{D} = v^\alpha D_\alpha$ and $\mathcal{D} = s^\alpha D_\alpha$ are linear combinations of the divisors D_α inherited from the base. To ensure the correct normalization of the simple root α_i these divisors have to satisfy the condition

$$\mathcal{B} \cdot S \cdot \tilde{D} \cdot \mathcal{D} = 1 . \tag{3.11}$$

Hence, for $D_i, \tilde{D}, \mathcal{D}$ being holomorphic hypersurfaces of \tilde{X}_4 the curves which correspond to the negative simple roots are effective curves and elements in the relative Mori cone. The situation is different for the weights. Some of the weights do not correspond to effective curves. However, if one finds a weight which corresponds to an effective curve, one can construct other weights corresponding to effective curves from a linear combination of the original weight and the negative simple roots with positive integer coefficients. This does not mean that all the weights correspond to effective curves since some weights need negative coefficients for their construction.

The co-dimension one singularities in \mathcal{B} over the surface S_b determine the gauge group G on the 7-branes. Generically, there are also co-dimension two and co-dimension three singularities. Physically, charged matter fields are localized on the co-dimension two singularities and the Yukawa interaction between these fields is generated from co-dimension three singularities. Focusing on G we realize that the Cartan divisors D_i are \mathbb{P}^1 -fibrations at the generic points in the surface S_b . However, the \mathbb{P}^1 -fibers may degenerate into smaller irreducible components along the singularity enhancement locus where the matter and Yukawa couplings are localized. The resolution of the co-dimension one singularity generates the extended Dynkin diagram of G . The resolution of the higher co-dimension singularity will generate another Dynkin diagram which may have a rank larger than $\text{rank}(G)$. We propose rules to determine the Dynkin diagrams from the resolution of the higher co-dimension singularity by exploiting the relative Mori cone.

Let us consider a situation where the charged matter fields in the representation of \mathbf{R} and \mathbf{R}^* of G are localized along the co-dimension two singularity enhancement locus $\Sigma_{\mathbf{R}}$. From the relative Mori cone, one can determine whether a weight of \mathbf{R} or \mathbf{R}^* corresponds to a effective curve or not. Then, the rule to determine the degeneration of \mathbb{P}^1 along $\Sigma_{\mathbf{R}}$

is that the negative of a simple root decomposes into a weight of \mathbf{R} and a weight of \mathbf{R}^* if both of them correspond to effective curves. If a curve corresponding to a weight lies in the relative Mori cone it is an effective curve. In this decomposition process one has to use the generators of the extended relative Mori cone as much as possible. In particular, one checks if the weight of \mathbf{R} found in the decomposition can be further decomposed into a weight of \mathbf{R} and the negative of a simple root, and if either of them is an element of the relative Mori cone or corresponds to the extended node. In this evaluation one should not mix with the weight of the other representation. Also, since the negative of a simple root is a generator of the relative Mori cone, it does not need to be decomposed further. By collecting all the irreducible components along $\Sigma_{\mathbf{R}}$ plus a curve corresponding to the extended Dynkin node, one can construct a Dynkin diagram generated from the resolution along the co-dimension two singularity locus $\Sigma_{\mathbf{R}}$. To make this algorithm more clear without introducing all the details of the global geometry we give a simple $SU(5)$ example in subsection 3.2.2.

The co-dimension three singularity enhancement occurs at a point p where at least two co-dimension two singularity loci intersect:

$$p = \Sigma_{\mathbf{R}} \cdot \Sigma_{\mathbf{R}'} \subset S_b . \quad (3.12)$$

Here we suppose that the charged matter fields in the representation of \mathbf{R} and \mathbf{R}^* localized on one curve $\Sigma_{\mathbf{R}}$, and other charged matter fields in the representation of \mathbf{R}' and \mathbf{R}'^* are localized along the other curve $\Sigma_{\mathbf{R}'}$. Although the Dynkin diagram obtained from the resolution along the locus $\Sigma_{\mathbf{R}}$ consists of some of the weights of \mathbf{R} , weights of \mathbf{R}^* and the negative simple roots, the weights of \mathbf{R}' and the weights of \mathbf{R}'^* can also form the nodes of the Dynkin diagram from the resolution at the co-dimension three singularity point p obtained (3.12). Hence, a weight of $\mathbf{R}, \mathbf{R}'^*$ or the negative of a simple root of G further decomposes at p if they are made of effective curves which correspond to any weights of $\mathbf{R}, \mathbf{R}^*, \mathbf{R}', \mathbf{R}'^*$ and the negative simple roots of G . When the singularity is enhanced to $G_p \supset G$ at p , this decomposition has to obey the algebra of G_p . From this decomposition rule, one can obtain all the weights and simple roots which form a Dynkin diagram obtained from the resolution of the co-dimension three singularity at p .

3.2.2 A simple $SU(5)$ example

Since this explanation is rather abstract, let us illustrate the above procedure on a simple example with gauge group $SU(5)$. The representations are the $\mathbf{R} = \mathbf{5}$, and $\mathbf{R} = \mathbf{10}$ along enhancement curves $\Sigma_{\mathbf{5}}$ and $\Sigma_{\mathbf{10}}$ respectively. We will not introduce the complete geometry here, but rather focus on the determination of the Dynkin nodes over the enhancement loci. In other words we assume the the ℓ -vectors have been determined for a given geometry, and the association of the generators of the relative Mori cone with the weights of $SU(5)$ has been performed. We consider the following identification:

$$\tilde{\ell}_1 \cong -e_3, \quad \tilde{\ell}_2 \cong e_3 + e_4, \quad \tilde{\ell}_3 \cong -e_1 + e_2, \quad \tilde{\ell}_4 \cong -e_2 - e_4 , \quad (3.13)$$

where $\tilde{\ell}_i$ are the ℓ -vectors generating the relative Mori cone, and e_i are a orthonormal basis of \mathbb{R}^5 allowing to represent the roots and weights for $SU(5)$ and its representations. A

compact Calabi-Yau fourfold which exactly yields the identification (3.13) can be found in section 4.1, see equation (4.5).

We first want to determine the weights which appear as curves in the relative Mori cone. For the weights of the **5** representation, $-e_3$ corresponds to an effective curve from the generators of the relative Mori cone (3.13). Then, it is straightforward to see

$$e_4 = (-e_3) + (e_3 + e_4), \quad (3.14)$$

$$-e_2 = (-e_2 - e_4) + (-e_3) + (e_3 + e_4), \quad (3.15)$$

$$-e_1 = (-e_1 + e_2) + (-e_2 - e_4) + (-e_3) + (e_3 + e_4). \quad (3.16)$$

Hence, e_4 , $-e_1$, and $-e_2$ correspond to effective curves. To determine e_5 or $-e_5$ corresponds to an effective curve, we use the fact that $e_1 + e_2 + e_3 + e_4 + e_5$ is a singlet of $SU(5)$. Then, we have

$$e_5 = e_1 + e_3 + e_5 + (-e_1) + (-e_3), \quad (3.17)$$

$$= (-e_2 - e_4) + (-e_1) + (-e_3). \quad (3.18)$$

Therefore, e_5 corresponds to an effective curve. To summarize, the correspondence between the effective curves and the **5** weights is given by

$$e_1 < 0, \quad e_2 < 0, \quad e_3 < 0, \quad e_4 > 0, \quad e_5 > 0, \quad (3.19)$$

and has to be interpreted using the notation (3.9). A similar analysis can be carried out for the weights of the **10** representation

$$e_1 + e_2 < 0, \quad e_1 + e_3 < 0, \quad e_2 + e_3 < 0, \quad e_2 + e_4 < 0, \quad (3.20)$$

$$e_3 + e_4 > 0, \quad e_3 + e_5 > 0, \quad e_4 + e_5 > 0.$$

This concludes the identification of weights with effective curves.

Using this information we can now determine how the negative simple roots degenerate over the enhancement curves $\Sigma_{\mathbf{10}}$ and $\Sigma_{\mathbf{5}}$. Let us start with $\Sigma_{\mathbf{10}}$, along which some of the negative simple roots degenerate into **10** and $\overline{\mathbf{10}}$ weights. First, we consider the decomposition of the negative simple roots into smaller components along $\Sigma_{\mathbf{10}}$

$$-(\text{simple root}) = \overline{\mathbf{10}} \text{ weight} + \mathbf{10} \text{ weight}. \quad (3.21)$$

Then, if both $\overline{\mathbf{10}}$ weights and **10** weights correspond to effective curves in the relative Mori cone, this degeneration occurs along $\Sigma_{\mathbf{10}}$. The check of effectiveness of the curves corresponding to all the **10** weights was given in (3.20). Hence, the degeneration of the negative simple roots along $\Sigma_{\mathbf{10}}$ are

$$-e_2 + e_3 = (-e_2 - e_4) + (e_3 + e_4), \quad (3.22)$$

$$-e_4 + e_5 = (-e_1 - e_4) + (e_1 + e_5) = (-e_1 + e_2) + (-e_2 - e_4) + (e_1 + e_5).$$

To summarize, along Σ_{10} the negative simple roots of $SU(5)$ plus the extended node $e_1 - e_5$ split into

$$e_1 - e_5, \quad e_1 + e_5, \quad -e_1 + e_2, \quad -e_2 - e_4, \quad -e_3 + e_4, \quad e_3 + e_4. \quad (3.23)$$

The resolution curves associated to the weights (3.23) form the extended Dynkin diagram of D_5 as depicted in Figure 2. Note that the well-known form of the D_5 Dynkin diagram is not directly visible by simply looking at the group-theoretic intersections of the elements (3.23). However, this structure can be inferred by a local analysis as presented in appendix C. Let us stress that this information is not needed in the evaluation of the chirality formulas and hence will not play a major role in this work.

We next turn to singularity enhancement locus $\Sigma_{\bar{5}}$. In this case, some of the negative simple roots decompose into $\mathbf{5}$ weight and $\bar{\mathbf{5}}$ weight,

$$-(\text{simple root}) = \bar{\mathbf{5}} \text{ weight} + \mathbf{5} \text{ weight}. \quad (3.24)$$

Since $-e_3$ and e_4 corresponds to the effective curves from (3.19), the decomposition of the negative simple roots along $\Sigma_{\bar{5}}$ is

$$-e_3 + e_4 = (-e_3) + (e_4). \quad (3.25)$$

Then, the negative simple roots of the $SU(5)$ plus the extended Dynkin node become

$$e_1 - e_5, \quad -e_1 + e_2, \quad -e_2 + e_3, \quad -e_3, \quad e_4, \quad -e_4 + e_5. \quad (3.26)$$

The curves associated to these weights form the extended A_5 Dynkin diagram as depicted in the Figure 2. Once again, we will only need in the derivation of the chirality formulas the identification of (3.26) with effective curves and not the precise match with the Dynkin diagram.

3.3 Matter surfaces and the chiral index

Having discussed how the relative Mori cone can determine the resolution process of the higher co-dimension singularities we next want to include the G_4 fluxes on \tilde{X}_4 and evaluate a chirality formula (2.1). Recall from section 2.2 that F-theory fluxes have to satisfy the conditions (2.16) and (2.18). The non-vanishing components of G_4 are captured by the matrices $\Theta_{\Lambda\Sigma}$ and $\Theta_{m\alpha}$ introduced in (2.19).

Let us turn to the determination of the matter surfaces $S_{\mathbf{R}}$ appearing in (2.1) by using the extended relative Mori cone. As discussed in [3, 5, 24, 13, 18] this matter surface should be obtained by fibering the resolution \mathbb{P}^1 's over the matter curve $\Sigma_{\mathbf{R}}$ with representation \mathbf{R} and \mathbf{R}^* . A relation of the matter surfaces with the weights of \mathbf{R} was stressed in [13]. The fiber $\mathcal{C}_{\mathbf{w}}$ corresponds to a weight \mathbf{w} of the representation \mathbf{R} . The curves $\mathcal{C}_{\mathbf{w}}$ are identical to the ones introduced in the resolution of the co-dimension two singularity locus $\Sigma_{\mathbf{R}}$. Hence, each curve $\mathcal{C}_{\mathbf{w}}$ can be determined from the relative Mori cone as discussed above. Such effective curves can be written by the triple intersection of divisors. We make the Ansatz

$$\mathcal{C}_{\mathbf{w}} = t_{\mathbf{w}}^{A\Sigma} D_A \cdot D_{\Sigma} \cdot \mathcal{D}, \quad \mathcal{D} = s^\alpha D_\alpha, \quad (3.27)$$

with some real coefficients $t_{\mathbf{w}}^{A\Sigma} = t_{\mathbf{w}}^A v^\Sigma$ which generally depend on the s^α . Here $v^\Sigma D_\Sigma$ is an exceptional divisor which contains the curve $\mathcal{C}_{\mathbf{w}}$. Let us note that we checked this Ansatz for our examples, and showed that it can always be satisfied. This includes the observation that there exists a divisor \mathcal{D} , that intersects the base \mathcal{B} in a divisor, which can be separated as in (3.27). For weights of representations of the gauge group G on $S_{\mathbf{b}}$, \mathcal{D} intersects $S_{\mathbf{b}}$ in a curve. It would be desirable to give a geometric proof that there always exists a representation of the class of $\mathcal{C}_{\mathbf{w}}$ of the form (3.27).

At least for $SU(N)$ gauge theories with matter in the fundamental and anti-symmetric representation, one can show that the curve $\mathcal{C}_{\mathbf{w}}$ can be generally written as (3.27) using a group theory argument. In the fundamental or anti-symmetric representation, all the Cartan charges of the highest weight are non-negative. On the other hand, the other weights have at least one negative Cartan charge. Hence, the Ansatz (3.27) might only be impossible if the highest weight appears as a generator of the relative Mori cone. For the other weights one can always choose a component D_Λ in the Ansatz (3.27) which has negative intersection number with the curve $\mathcal{C}_{\mathbf{w}}$. If the highest weight is a generator of the relative Mori cone, all the weights correspond to effective curves in the relative Mori cone since the negative simple roots are always effective curves by (3.10). When one sums up all the weight e_i , ($i = 1, \dots, N$) in the fundamental representation, or the weights $e_i + e_j$, ($1 \leq i \neq j \leq N$) in the anti-symmetric representation, one has $N(e_1 + \dots + e_N)$ or $(N-1)(e_1 + \dots + e_N)$ respectively. Namely, the singlet of $SU(N)$ corresponds to the effective curve in the relative Mori cone. However, if the curve corresponding to the singlet is in the relative Mori cone, the relative Kähler cone cannot be defined since $\int_{\mathcal{C}_{\text{singlet}}} \sum s^i D_i = 0$. Therefore, the highest weight cannot be the generator of the relative Mori cone and the generators of the relative Mori cone should have at least one negative Cartan charge. This negative Cartan charge indicates that the curve is contained in an exceptional divisor. Hence, one can always make the Ansatz (3.27) for the $SU(N)$ gauge theories with matter in the fundamental and anti-symmetric representations.

Since our final interest is in the matter surface $S_{\mathbf{R}}$ we still have to extract a surface out of the curve (3.27). In order to do that we propose to pull out the divisor \mathcal{D} which becomes a curve in $S_{\mathbf{b}}$. In order that the normalization of the $t_{\mathbf{w}}^{A\Sigma}$ in (3.27) is fixed we demand that the curve $\mathcal{D} \cdot S \cdot B$ intersects exactly once with the matter curve $\Sigma_{\mathbf{R}}$ in $S_{\mathbf{b}}$. In other words we normalize \mathcal{D} such that

$$\Sigma_{\mathbf{R}} \cdot \mathcal{D} = 1 . \quad (3.28)$$

The condition (3.28) fixes the normalization of \mathcal{D} , and via (3.27) the normalization of the $t_{\mathbf{w}}^{A\Sigma}$. The class of the matter surface $S_{\mathbf{R}}$ is then fixed and given by

$$S_{\mathbf{R}} = t_{\mathbf{w}}^{A\Sigma} D_A \cdot D_\Sigma , \quad (3.29)$$

with $t_{\mathbf{w}}^{A\Sigma} = t_{\mathbf{w}}^A v^\Sigma$ as in (3.27). For a fixed \mathcal{D} the parameters $t_{\mathbf{w}}^{A\Sigma}$ are determined from the intersection numbers between the curve $\mathcal{C}_{\mathbf{w}}$ and the divisors D_A . The intersection numbers are already known as entries of the ℓ -vectors. This procedure does not determine the parameters uniquely, but fixes the class of the curve $\mathcal{C}_{\mathbf{w}}$ and the matter surface $S_{\mathbf{R}}$. Curves

are in the same class if their intersection number with the divisors are identical. Strictly speaking one should note that $S_{\mathbf{R}}$ depends on the chosen weight for the representation \mathbf{R} . However, as will become more clear momentarily, this ambiguity drops out from the chirality formula (2.1).

Using the non-vanishing components of the G_4 flux (2.19), the chirality formula (2.1) together with the explicit form of the matter surfaces $S_{\mathbf{R}}$ (3.29) yields

$$\chi(\mathbf{R}) = t_{\mathbf{w}}^{A\Sigma} \Theta_{A\Sigma} . \quad (3.30)$$

From this expression one can infer that the chirality is indeed independent of the weight \mathbf{w} and only depends on the representation \mathbf{R} . Suppose that a curve corresponding to another weight \mathbf{w}' of the representation \mathbf{R} also appears along the locus $\Sigma_{\mathbf{R}}$. Since any two weights can be related by a linear combination of simple roots, one can write $\mathbf{w}' = \mathbf{w} - \sum_i u^i \alpha_i$. Since the negative simple roots can be always written as (3.10), we can expand $\tilde{D} = v^\alpha D_\alpha$, and identify \mathcal{D} of (3.10) and (3.27). Hence, adding or subtracting the negative simple roots to or from the weight \mathbf{w} corresponds to adding or subtracting $D_i \cdot \tilde{D}$ to or from $t_{\mathbf{w}}^{A\Sigma} D_A \cdot D_\Sigma$. Then, the expression (3.30) evaluated for the two different weights \mathbf{w} and \mathbf{w}' yields

$$\begin{aligned} t_{\mathbf{w}'}^{A\Sigma} \Theta_{A\Sigma} &= t_{\mathbf{w}}^{A\Sigma} \Theta_{A\Sigma} + u^i v^\alpha \Theta_{i\alpha} \\ &= t_{\mathbf{w}}^{A\Sigma} \Theta_{A\Sigma} , \end{aligned} \quad (3.31)$$

where we use (2.18). Therefore, the chirality formula (3.30) does not depend on the weight \mathbf{w} but only on the representation \mathbf{R} . In geometrical terms this also implies that (3.30) does not depend on the topological phases of the \tilde{X}_4 distinguishing different Calabi-Yau resolutions of X_4 . In fact, in different phases other weights of the same representation are associated to the matter curves, and (3.31) ensures independency of the resolution phase.

4. Examples

In this section we discuss two illustrative examples of explicitly resolved Calabi-Yau hypersurfaces realized in a toric ambient space. Our first example will admit an $SU(5)$ singularity over a divisor in the base, as in the torically realized GUT models of [10, 11]. In the second example an additional $U(1)$ will be present, such that $n_{U(1)} = 1$ in (2.6). The toric construction will correspond to the $U(1)$ -restricted Tate model of [8]. The toric methods required to perform the computations of this subsection have been explained in [14, 15, 10, 11], and were recently reviewed in [42]. The determination of the Mori cone can be performed using the methods of [39, 40, 41] as reviewed in appendix B.

4.1 A Calabi-Yau hypersurface with $SU(5)$ gauge group

As the first example, we consider a Calabi-Yau fourfold \tilde{X}_4 which has a K3 fibration. The K3 fibration itself has an elliptic fibration such that it can be used in an F-theory

compactification. Such a Calabi–Yau fourfold can be obtained from a hypersurface in the ambient toric space whose points on edges of the polyhedron are

points	divisor basis
-1 0 0 0 0	D_1
0 -1 0 0 0	D_2
3 2 0 0 0	$D_3 = \mathcal{B}$
3 2 1 0 0	$D_4 = \hat{S}$
3 2 -1 0 0	D_5
3 2 0 1 1	D_6
3 2 0 -1 0	D_7
3 2 0 0 -1	$D_8 = H$
2 1 1 0 0	$D_9 = B_1$
1 1 1 0 0	$D_{10} = B_2$
1 0 1 0 0	$D_{11} = B_3$
0 0 1 0 0	$D_{12} = B_4$

(4.1)

Note that we have introduced a basis of independent toric divisors \mathcal{B}, \hat{S}, H , and B_i . These 7 divisors will span a basis of independent divisors on a generic hypersurface \tilde{X}_4 embedded in the class $K = \sum_i D_i$, such that $h^{1,1}(\tilde{X}_4) = 7$.⁷ One realizes from (4.1) that $S_b = \mathcal{B} \cdot \hat{S}$ is the \mathbb{P}^2 base of the K3-fibration. The normal bundle $N_{S_b|\mathcal{B}}$ is trivial $N_{S|\mathcal{B}} = \mathcal{O}_{\mathbb{P}^2}$. In (4.1) we also introduced the blow up divisors B_i for the resolution of an A_4 singularity over S_b . The to S_b associated divisor \hat{S} in \tilde{X}_4 is given by $S = \hat{S} + B_1 + B_2 + B_3 + B_4$ as an $SU(5)$ version of (2.4). The Hodge numbers of the Calabi–Yau fourfold can be computed as

$$h^{1,1}(\tilde{X}_4) = 7, \quad h^{2,1}(\tilde{X}_4) = 0, \quad h^{3,1}(\tilde{X}_4) = 2148, \quad \chi(\tilde{X}_4) = 12978. \quad (4.2)$$

4.1.1 Mori cone, resolutions and group theory

The generators of the Mori cone for the Calabi–Yau fourfold \tilde{X}_4 can be obtained by the method described in [39, 40, 41]. Note that the generators of the Mori cone for a toric ambient space is generally different from the generators of the Mori cone for a Calabi–Yau fourfold hypersurface. In general, some of the triangulations for the ambient space are connected by a flop of a curve which is not inside the Calabi–Yau fourfold. In our case, we have 54 star-triangulations of the polyhedron (4.1) from the origin. However some of them are connected by the flops of the curves which are not included in \tilde{X}_4 . If the defining equation of a curve and the Calabi–Yau hypersurface \tilde{X}_4 cannot be satisfied simultaneously because they are elements of the Stanley-Reisner ideal, the flop of the curve is not a true flop in the Calabi–Yau fourfold \tilde{X}_4 . This can be confirmed from the distinct intersection numbers of \tilde{X}_4 since different phases give different intersection numbers. In the derivation of the intersection numbers we use the star-triangulations ignoring the interior points in

⁷This is a consequence of the Lefschetz hyperplane theorem.

the facets. The presence of these points indicates the existence of point-like singularities in the ambient space. Since the Calabi–Yau hypersurface does generically not intersect these singularities, a star-triangulation of the points in the polyhedron (4.1) yields a smooth Calabi–Yau hypersurface. In our example (4.1), we find that the true number of the triangulations for \tilde{X}_4 is three. The generators of the Mori cone for the three phases are:

phase I								phase II								phase III							
ℓ_1	ℓ_2	ℓ_3	ℓ_4	ℓ_5	ℓ_6	ℓ_7		ℓ_1	ℓ_2	ℓ_3	ℓ_4	ℓ_5	ℓ_6	ℓ_7		ℓ_1	ℓ_2	ℓ_3	ℓ_4	ℓ_5	ℓ_6	ℓ_7	
0	0	0	1	0	0	0		0	0	0	1	0	0	0		0	0	0	1	0	0	0	
0	0	0	0	1	0	0		0	0	0	0	1	0	0		0	0	0	0	1	0	0	
-2	-3	1	0	0	0	0		-2	-3	1	0	0	0	0		-2	-3	1	0	0	0	0	
1	0	-2	0	0	1	0		1	0	-2	0	0	1	0		1	0	-1	1	0	1	-1	
1	0	0	0	0	0	0		1	0	0	0	0	0	0		1	0	0	0	0	0	0	
0	1	0	0	0	0	0		0	1	0	0	0	0	0		0	1	0	0	0	0	0	
0	1	0	0	0	0	0		0	1	0	0	0	0	0		0	1	0	0	0	0	0	
0	1	0	0	0	0	0		0	1	0	0	0	0	0		0	1	0	0	0	0	0	
0	0	1	0	0	-2	1		0	0	1	1	1	-1	-1		0	0	0	0	1	-2	1	
0	0	1	0	1	0	-1		0	0	1	-1	0	-1	1		0	0	0	-2	0	0	1	
0	0	0	1	-1	1	-1		0	0	0	0	-2	0	1		0	0	0	0	-2	1	0	
0	0	0	-1	0	0	1		0	0	0	0	1	1	-1		0	0	1	1	1	0	-1	

(4.3)

In the following we will indicate the phase by writing $\ell_i^{(I)}$, $\ell_i^{(II)}$, and $\ell_i^{(III)}$ for the Mori vectors of the three phases respectively. Note that

$$\ell_1^{(I)} = \ell_1^{(II)} = \ell_1^{(III)}, \quad \ell_2^{(I)} = \ell_2^{(II)} = \ell_2^{(III)}, \quad \ell_3^{(I)} = \ell_3^{(II)} = \ell_3^{(III)} + \ell_7^{(III)}. \quad (4.4)$$

From this identification we already realize that the phase III will be special, since its ℓ -vectors appear more non-trivially in the last identification.

A subset of the generators of the Mori cone for each phase corresponds to effective curves and can be identified with weights in a representation of $SU(5)$ in the way described in the section 3.2. One can read off the Cartan matrix C_{ij} from the intersection numbers (2.13). By comparing it with the Cartan matrix of $SU(5)$, one can deduce that the blow up divisors B_1, B_2, B_3, B_4 correspond to the simple roots $e_1 - e_2, e_4 - e_5, e_2 - e_3, e_3 - e_4$ respectively. Here e_i denotes the orthonormal basis of \mathbb{R}^5 . Then, we can identify the generators of the Mori cone (4.3) with the weights of some representations of $SU(5)$ from the Cartan charges (3.6). Since we are interested in the extended relative Mori cone, the relevant generators for the phase I is $\ell_3^{(I)}, \ell_4^{(I)}, \ell_5^{(I)}, \ell_6^{(I)}, \ell_7^{(I)}$. Among them the generators of the relative Mori cone (3.2) have negative intersection numbers with the Cartan divisors. Hence, they are $\ell_4^{(I)}, \ell_5^{(I)}, \ell_6^{(I)}, \ell_7^{(I)}$ and $\ell_3^{(I)}$ corresponds to the extended Dynkin node. The weights of the generators of the relative Mori cone for the phase I are

$$\ell_4^{(I)} \cong -e_3, \quad \ell_5^{(I)} \cong e_3 + e_4, \quad \ell_6^{(I)} \cong -e_1 + e_2, \quad \ell_7^{(I)} \cong -e_2 - e_4. \quad (4.5)$$

The extended node $\ell_3^{(I)}$ corresponds to $e_1 - e_5$. For the phase II, the generators of the relative Mori cone are $\ell_4^{(II)}, \ell_5^{(II)}, \ell_6^{(II)}, \ell_7^{(II)}$. They correspond to the following weights

$$\ell_4^{(II)} \cong e_1 + e_5, \quad \ell_5^{(II)} \cong -e_2 + e_3, \quad \ell_6^{(II)} \cong -e_1 - e_4, \quad \ell_7^{(II)} \cong e_2 + e_4. \quad (4.6)$$

$e_1 + e_2 < 0$	$e_1 + e_2 < 0$	$e_1 + e_2 < 0$
$e_1 + e_3 < 0$	$e_1 + e_3 < 0$	$e_1 + e_3 < 0$
$e_2 + e_3 < 0$ $e_1 + e_4 < 0$	$e_2 + e_3 < 0$ $e_1 + e_4 < 0$	$e_2 + e_3 < 0$ $e_1 + e_4 > 0$
$e_2 + e_4 < 0$ $e_1 + e_5 > 0$	$e_2 + e_4 > 0$ $e_1 + e_5 > 0$	$e_2 + e_4 > 0$ $e_1 + e_5 > 0$
$e_3 + e_4 > 0$ $e_2 + e_5 > 0$	$e_3 + e_4 > 0$ $e_2 + e_5 > 0$	$e_3 + e_4 > 0$ $e_2 + e_5 > 0$
$e_3 + e_5 > 0$	$e_3 + e_5 > 0$	$e_3 + e_5 > 0$
$e_4 + e_5 > 0$	$e_4 + e_5 > 0$	$e_4 + e_5 > 0$
Phase I	Phase II	Phase III

Figure 1: The effective curves corresponding to the weights of **10** representation. The negative sign means that the negative of the weight corresponds to a effective curve.

Similarly, $\ell_3^{(\text{II})}$ corresponds to the extended Dynkin node $e_1 - e_5$, and $\ell_3^{(\text{II})}, \ell_4^{(\text{II})}, \ell_5^{(\text{II})}, \ell_6^{(\text{II})}, \ell_7^{(\text{II})}$ are the generators of the extended relative Mori cone. For the phase III, the generators of the relative Mori cone and their correspondence to the weights are

$$\ell_4^{(\text{III})} \cong -e_4 + e_5, \quad \ell_5^{(\text{III})} \cong -e_2 + e_3, \quad \ell_6^{(\text{III})} \cong -e_1 + e_2, \quad \ell_7^{(\text{III})} \cong e_1 + e_4. \quad (4.7)$$

In this phase, we have a generator $\ell_3^{(\text{III})}$ which corresponds to a weight $-e_4 - e_5$ and does not shrink to a point in X_4 . Hence $\ell_3^{(\text{III})}, \ell_4^{(\text{III})}, \ell_5^{(\text{III})}, \ell_6^{(\text{III})}, \ell_7^{(\text{III})}$ are the generators of the extended relative Mori cone.

So far we have determined the generators of the extended relative Mori cone. This implies that the weights (4.5)–(4.7) correspond to effective curves. Using the strategy of section 3.2 one can also determine whether other weights correspond to effective curves from the relative Mori cone. Comparing (4.5) and (3.13) we note that section 3.2.2 precisely discusses the phase I of the resolved Calabi-Yau fourfold (4.1). The identification of the effective curves was given in (3.19). Following the same strategy also for phases II and III, one shows that for all the three phases one has

$$e_1 < 0, \quad e_2 < 0, \quad e_3 < 0, \quad e_4 > 0, \quad e_5 > 0. \quad (4.8)$$

where we use the notation (3.9). In section 3.2.2 also the determination of the effectiveness of the **10** weights has been given for phase I. The result was given in (3.20). Repeating the same analysis for the phases II and III one finds the result summarized in Figure 1.

As also explained in section 3.2, one next determines the weights which describe the curves fibering over the matter curves Σ_5 and Σ_{10} . This allows to determine the degeneration structure of the curves in the Cartan resolution divisors D_i from the relative Mori

cone. One considers the splits

$$\Sigma_{\mathbf{10}} : \quad -(\text{simple root}) = \overline{\mathbf{10}} \text{ weight} + \mathbf{10} \text{ weight} , \quad (4.9)$$

$$\Sigma_{\mathbf{5}} : \quad -(\text{simple root}) = \overline{\mathbf{5}} \text{ weight} + \mathbf{5} \text{ weight} . \quad (4.10)$$

For the phase I this was explained in detail in section 3.2.2. The result was that the weights corresponding to the matter curves $\Sigma_{\mathbf{10}}$ and $\Sigma_{\mathbf{5}}$ are

$$\Sigma_{\mathbf{10}} : \quad e_1 - e_5, e_1 + e_5, -e_1 + e_2, -e_2 - e_4, -e_3 + e_4, e_3 + e_4 , \quad (4.11)$$

$$\Sigma_{\mathbf{5}} : \quad e_1 - e_5, -e_1 + e_2, -e_2 + e_3, -e_3, e_4 - e_4 + e_5, \quad (4.12)$$

as shown in (3.23) and (3.26). The weights (4.11) form the extended Dynkin diagram of D_5 in Figure 2. Similarly, the weights (4.12) form the extended A_5 Dynkin diagram also depicted in Figure 2. The intersection numbers for both Dynkin diagrams can be calculated from the direct computation in appendix C. We will not need these intersection numbers in the following.

4.1.2 Yukawa couplings at co-dimension three

We have studied the degeneration along the co-dimension-two singularity locus. The singularity further enhances along the E_6 and D_6 Yukawa points. At the Yukawa points, the curves of (4.11) and (4.12) further degenerate into smaller irreducible components. In this case, the degeneration generates the curves corresponding to $\mathbf{10}$, $\overline{\mathbf{10}}$ weights and also $\mathbf{5}$, $\overline{\mathbf{5}}$ weights from one Yukawa point. In general, when the singularity is enhanced to G_p at the co-dimension-three point, our proposal is that the degeneration of the curves obeys the algebra of G_p . Namely, the further degeneration is possible only if the decompositions of the weights at E_6 and D_6 points obey the E_6 and D_6 algebra respectively. First, let us see the degeneration of the extended D_5 Dynkin diagram at the E_6 enhancement point. Since $e_1 - e_5$, $-e_1 + e_2$, $-e_2 - e_4$, $e_3 + e_4$ correspond to the generators of the relative Mori cone, they do not degenerate further. Since $\mathbf{5}$ or $\overline{\mathbf{5}}$ weights can appear at the E_6 enhancement point, the negative simple root $-e_3 + e_4$ in (4.11) can decompose as

$$-e_3 + e_4 = (-e_3) + (e_4). \quad (4.13)$$

Moreover, we have the decomposition

$$\begin{aligned} e_1 + e_5 &= -e_2 - e_3 - e_4, \\ &= (-e_2 - e_4) + (-e_3). \end{aligned} \quad (4.14)$$

We use the fact that $e_1 + e_2 + e_3 + e_4 + e_5$ is a singlet in $SU(5)$. The decomposition (4.13) obviously obeys the E_6 algebra since the adjoint weight decomposes into a vector-like pair. In order to see that the decomposition (4.14) obeys the algebra of E_6 but does not obey

the algebra of D_6 , one can consider the following decomposition

$$E_6 \supset SU(5) \times U(1)_1 \times U(1)_2 \quad (4.15)$$

$$\begin{aligned} \mathbf{78} \rightarrow & \mathbf{1}_{0,0} + \mathbf{1}_{0,0} + \mathbf{1}_{-5,-3} + \mathbf{1}_{5,3} + \mathbf{24}_{0,0} \\ & + \mathbf{5}_{-3,3} + \mathbf{\bar{5}}_{3,-3} + \mathbf{10}_{-1,-3} + \mathbf{\bar{10}}_{1,3} + \mathbf{10}_{4,0} + \mathbf{\bar{10}}_{-4,0}, \end{aligned}$$

$$D_6 \supset SU(5) \times U(1)_1 \times U(1)_2 \quad (4.16)$$

$$\begin{aligned} \mathbf{66} \rightarrow & \mathbf{1}_{0,0} + \mathbf{1}_{0,0} + \mathbf{24}_{0,0} \\ & + \mathbf{5}_{2,2} + \mathbf{5}_{-2,-2} + \mathbf{\bar{5}}_{-2,2} + \mathbf{\bar{5}}_{-2,-2} + \mathbf{10}_{4,0} + \mathbf{\bar{10}}_{-4,0}. \end{aligned}$$

From the E_6 decomposition (4.15), one can associate the E_6 algebra

$$\mathbf{10}_{4,0} \rightarrow \mathbf{\bar{10}}_{1,3} + \mathbf{\bar{5}}_{3,-3} \quad (4.17)$$

to (4.14). However, one cannot associate the D_6 algebra to (4.14) since the $U(1)$ charges are not conserved under the decomposition. Hence, this degeneration corresponds to the E_6 enhancement point. To summarize, we have the weights

$$e_1 - e_5, \quad -e_1 + e_2, \quad -e_2 - e_4, \quad e_3 + e_4, \quad -e_3, \quad e_4, \quad (4.18)$$

at the E_6 Yukawa point. The weights (4.18) form the E_6 Dynkin diagram depicted in Figure 2. As noted in [20], (4.18) does not form the ‘extended’ E_6 diagram and the rank does not enhances at the E_6 Yukawa point.

One can also do the same analysis for the degeneration of the extended D_5 Dynkin diagram at the a D_6 enhancement point. At the D_6 Yukawa point, the degeneration of (4.14) is impossible since it does not satisfy the D_6 algebra. Hence, $e_1 + e_5$ remains to be irreducible at the D_6 Yukawa point. On the other hand, $-e_3 + e_4$ can decompose differently to (4.13) as

$$-e_3 + e_4 = (-e_3) + (-e'_3) + (e_3 + e_4). \quad (4.19)$$

The decomposition (4.19) is possible for the D_6 enhancement point since one has two $\mathbf{\bar{5}}$ representations with different charges under $U(1)_1 \times U(1)_2$ in the decomposition of $SO(12)$ as displayed in (4.16). The $U(1)$ charge conservation corresponding to (4.19) becomes

$$\mathbf{24}_{0,0} \rightarrow \mathbf{\bar{5}}_{-2,2} + \mathbf{\bar{5}}_{-2,-2} + \mathbf{10}_{4,0}. \quad (4.20)$$

This is not allowed in the E_6 algebra. Note that our proposal is that one has to decompose the weights into the generators of the extended relative Mori cone as much as possible. Therefore, the degeneration at the D_6 Yukawa point should not stop at (4.13) but proceeds further to (4.19) since both $-e_3$ and $e_3 + e_4$ are the generators of the extended relative Mori cone. To summarize, we have the weights

$$e_1 - e_5, \quad e_1 + e_5, \quad -e_1 + e_2, \quad -e_2 - e_4, \quad e_3 + e_4, \quad -e_3, \quad -e'_3. \quad (4.21)$$

at the D_6 Yukawa point. The curves associated to (4.21) form the extended D_6 Dynkin diagram in Figure 2.

The chains of the Dynkin diagrams for the phase II and III can be computed in a similar manner and they are depicted in Figures 4 and 5.

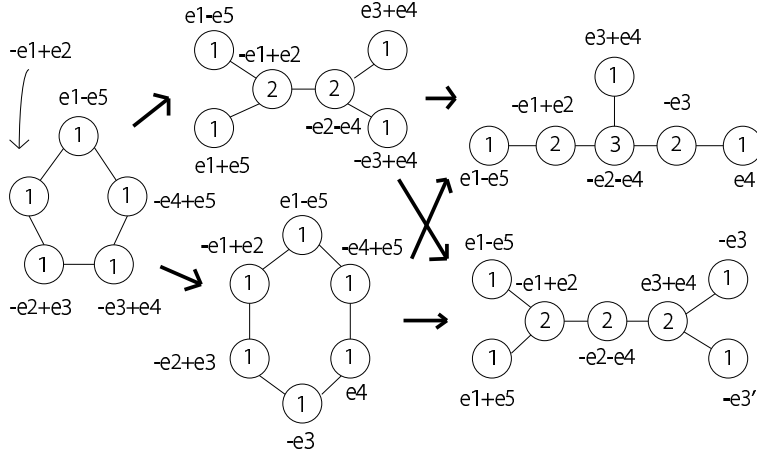


Figure 2: The chain of the Dynkin diagrams for the phase I. The number in the nodes denotes the multiplicity. The intersection structure cannot be inferred by simple group theoretic arguments about the weights, but requires an inspection of the resolution geometry.

4.1.3 G_4 -flux and chirality

In this section we test the chirality formula (2.1) for the matter fields in the $\mathbf{10}$ and $\bar{\mathbf{5}}$ representation from the F-theory compactifications on the Calabi–Yau fourfold (4.41). The necessary information is the G_4 flux and the matter surfaces $S_{\mathbf{R}}$ for the $\mathbf{10}$ and $\bar{\mathbf{5}}$ matter fields. Hereafter, we also focus on the phase I. A construction of the G_4 flux and matter surfaces for $SU(5)$ examples can be also be found in [13].

First we determine G_4 flux. We consider the G_4 flux constructed from the intersection of the divisors of \tilde{X}_4 . In order to preserve four-dimensional Poincaré invariance and the $SU(5)_{GUT}$ symmetry, the G_4 flux should satisfy the conditions (2.18). We find such G_4 flux from the expansion by the general intersection of the divisors. Without any constraint, we have $7 \times 8/2 = 28$ generators of such surfaces. However, not all of them are independent. First of all, we have the constraints from the Stanley-Reisner ideal of the toric ambient space for \tilde{X}_4 . For the phase I, the Stanley-Reisner ideal is

$$SR = \{D_2D_{10}, D_3D_9, D_3D_{10}, D_3D_{11}, D_3D_{12}, D_4D_5, D_4D_{11}, D_4D_{12}, D_1D_9, D_1D_{11}, D_5D_9, D_5D_{10}, D_5D_{11}, D_5D_{12}, D_9D_{12}, D_1D_2D_3, D_1D_2D_4, D_6D_7D_8\}. \quad (4.22)$$

Hence we have 15 constraints for the surfaces and all of them are independent. We have another constraints coming from the incompatibility between the Stanley-Reisner ideal and the Calabi–Yau hypersurface equation. Those constraints are

$$D_1D_3, D_1D_4, D_2D_3, D_2D_4, D_2D_9. \quad (4.23)$$

However, not all the constraints from (4.22) and (4.23) are independent. There are actually 19 independent constraints in total, so the number of the true generators for the expansion of surfaces is $28 - 19 = 9$. We choose

$$B_4^2, B_3 \cdot B_4, B_3^2, B_2 \cdot B_3, B_2^2, B_4 \cdot H, H^2, H \cdot \hat{S}, B \cdot H \quad (4.24)$$

Then, the general expansion of the G_4 flux by the nine independent surfaces is

$$G_4 = \alpha_1 B_4^2 + \alpha_2 B_3 \cdot B_4 + \alpha_3 B_3^2 + \alpha_4 B_2 \cdot B_3 + \alpha_5 B_2^2 + \alpha_6 B_4 \cdot H + \alpha_7 H^2 + \alpha_8 H \cdot \hat{S} + \alpha_9 \mathcal{B} \cdot H. \quad (4.25)$$

The condition (2.18) reduces the nine parameters to one parameter,

$$G_4 = \beta(8B_2 \cdot B_3 - 4B_3 \cdot B_3 - 2B_3 \cdot B_4 + 3B_4^2 + 9B_4 \cdot H), \quad (4.26)$$

where $3\beta = \alpha_2$. We choose β such that all the coefficients are integers.

Let us turn to the matter surface $S_{\mathbf{10}}$ and $S_{\overline{\mathbf{10}}}$. From Figure 2, the matter surface $S_{\mathbf{10}}$ corresponds to the weights $e_1 + e_5, e_3 + e_4$, and $S_{\overline{\mathbf{10}}}$ corresponds to the weight $-e_2 - e_4$. The class of the curves corresponding to $e_1 + e_5, e_3 + e_4$ and $-e_2 - e_4$ can be determined from the intersection numbers (4.3). For example, let us consider a curve ℓ_7 corresponding to the weight $-e_2 - e_4$. Since our final interest is the matter surface, we have to pull out a divisor, which intersects S_b in a curve, from the triple intersection representing the curve. We make the Ansatz $(\mu H + \nu S)$ for this divisor. Furthermore, when ℓ_i has a negative intersection number with a divisor B_i , the triple intersection representing ℓ_i has a component B_i . Hence, we can make a general Ansatz for ℓ_7 , $\ell_7 = aB_2 \cdot B_3 \cdot (\mu H + \nu S)$. The parameter a can be determined from the intersection numbers and the result is

$$\overline{\mathbf{10}}: \quad \ell_7^{(1)} \cong -e_2 - e_4 \quad \rightarrow \quad \frac{1}{3\mu} B_2 \cdot B_3 \cdot (\mu H + \nu S). \quad (4.27)$$

Note that we solve only for a and not for μ and ν in this process. In order to obtain a matter surface corresponding to the weight $-e_2 - e_4$, one has to pull out a divisor in \mathcal{B} with a correct multiplicity. The correct multiplicity can be determined from the intersection with the matter curve $\Sigma_{\mathbf{10}}$ (3.28). Since the $\mathbf{10}$ matter curve lies in the class $c_1(\mathcal{B})|_{S_b}$, (3.28) becomes

$$S_b \cdot_{\mathcal{B}} c_1(\mathcal{B}) \cdot_{\mathcal{B}} \mathcal{D} = 1. \quad (4.28)$$

In this case, the divisor can be chosen to be $\mathcal{D} = \frac{1}{3\mu}(\mu H + \nu S)$. Hence the matter surface $S_{\overline{\mathbf{10}}}$ corresponding to the weight $-e_2 - e_4$ is

$$S_{\overline{\mathbf{10}}} = B_2 \cdot B_3. \quad (4.29)$$

From this expression of the matter surface $S_{\overline{\mathbf{10}}}$, and the G_4 flux (4.26) one can compute the chirality for the $\mathbf{10}$ matter fields. The chirality formula (2.1) becomes

$$\chi(\overline{\mathbf{10}}) = \int_{S_{\overline{\mathbf{10}}}} G_4 = 3 \cdot 54\beta. \quad (4.30)$$

where we have used the intersection numbers of \tilde{X}_4 .

For the chirality formula of the $\bar{\mathbf{5}}$ matter, one has to determine the matter surface $S_{\bar{\mathbf{5}}}$. We consider a curve corresponding to the weight $-e_3$ which is one of the generators of the relative Mori cone for the phase I. From the intersections one can determine the class of the curve ℓ_4 corresponding to the weight $-e_3$. We also make an Ansatz such that the triple intersection has a component $(\mu H + \nu S)$ which is then being dropped in the determination

of the matter surface $S_{\bar{\mathbf{5}}}$. Moreover, since ℓ_4 has a negative intersection number with B_4 , we can make a general Ansatz $\ell_4 = (\sum_A a^A D_A) \cdot B_4 \cdot (\mu H + \nu S)$, where $\sum_A a^A D_A$ is a general linear combination of the divisors in (4.1). The parameters a_i can be determined from the intersection numbers, such that ℓ_4 is represented by

$$\bar{\mathbf{5}}: \ell_4^{(I)} \cong -e_3 \quad \rightarrow \quad \frac{1}{24\mu}(B_2 - B_3 + 9H) \cdot B_4 \cdot (\mu H + \nu S), \quad (4.31)$$

where we choose a special representative in the solutions just for the simplicity of the expression. In order to obtain the matter surface $S_{\bar{\mathbf{5}}}$, one has to pull out a divisor \mathcal{D} which satisfies the condition

$$S \cdot_{\mathcal{B}} (8c_1(\mathcal{B}) - 5S) \cdot_{\mathcal{B}} \mathcal{D} = 1, \quad (4.32)$$

where $(8c_1(\mathcal{B}) - 5S)|_S$ is a class of the $\bar{\mathbf{5}}$ matter curve. By using the condition (4.32), one finds \mathcal{D} being of the form $\mathcal{D} = \frac{1}{24\mu}(\mu H + \nu S)$. Hence the matter surface $S_{\bar{\mathbf{5}}}$ is

$$S_{\bar{\mathbf{5}}} = (B_2 - B_3 + 9H) \cdot B_4. \quad (4.33)$$

Therefore, the chirality formula for the $\bar{\mathbf{5}}$ matter becomes

$$\chi(\bar{\mathbf{5}}) = \int_{S_{\bar{\mathbf{5}}}} G_4 = -3 \cdot 54\beta, \quad (4.34)$$

where we have inserted the matter surface (4.33) and the flux (4.26), and used the intersection numbers of \tilde{X}_4 . From (4.30) and (4.34) we find the relation $\chi(\mathbf{10}) = -\chi(\overline{\mathbf{10}}) = \chi(\bar{\mathbf{5}})$, which is consistent with the anomaly conditions for $SU(5)$ gauge theories. Note that we did not discuss the quantization of β appearing in (4.30) and (4.34). This can be done by investigating the integrality properties of the basis used in (4.26), and satisfying the constraint (2.16).

4.1.4 Relation to three-dimensional Chern-Simons term

One can also see that the chirality (4.30) and (4.34) can be obtained from the formula (2.26). The sign in (2.28) is determined from the relative Mori cone. The effectiveness of the curves corresponding to $\mathbf{10}$ weights is depicted in the first column of Figure 1. The effectiveness of the curves corresponding to $\mathbf{5}$ weights is (4.8). The $U(1)_i$ charges $(q_f)_i$ of each weight can be determined from (3.6). By inserting all the information, the formula (2.26) for the Calabi–Yau fourfold (4.1) in the phase I is

$$\begin{aligned} \Theta_{23} &= -\chi(\mathbf{10}), & \Theta_{24} &= \frac{1}{2}\chi(\mathbf{10}) + \frac{1}{2}\chi(\bar{\mathbf{5}}), \\ \Theta_{33} &= \chi(\bar{\mathbf{5}}), & \Theta_{44} &= -\chi(\mathbf{10}), \\ \Theta_{13} &= \frac{1}{2}\chi(\mathbf{10}) - \frac{1}{2}\chi(\bar{\mathbf{5}}), & \Theta_{34} &= \frac{1}{2}\chi(\mathbf{10}) - \frac{1}{2}\chi(\bar{\mathbf{5}}) \\ \Theta_{11} &= -\chi(\mathbf{10}) + \chi(\bar{\mathbf{5}}), & \Theta_{22} &= \chi(\mathbf{10}) - \chi(\bar{\mathbf{5}}) \end{aligned} \quad (4.35)$$

and the other components are zero. Using the intersection numbers with the G_4 -flux (4.26), one can explicitly compute the components Θ_{ij} . One finds

$$\Theta_{23} = 3 \times 54\beta, \quad \Theta_{24} = -3 \times 54\beta, \quad \Theta_{33} = -3 \times 54\beta, \quad \Theta_{44} = 3 \times 54\beta, \quad (4.36)$$

with all the others being zero. By inserting the explicit numbers (4.36) into (4.35), one obtains

$$\chi(\mathbf{10}) = -3 \times 54\beta, \quad \chi(\bar{\mathbf{5}}) = -3 \times 54\beta. \quad (4.37)$$

This precisely matches the chirality obtained from integrating G_4 -fluxes over the matter surfaces (4.30) and (4.34).

4.1.5 Comparison with spectral cover

We compare the results of the proposed chirality formula (4.30) and (4.34) with the spectral cover computation. The chirality formula for the matter in $\mathbf{10}$ representation is [43, 44]

$$n_{\mathbf{10}} = -\lambda\eta \cdot (5K_{S_b} + \eta), \quad (4.38)$$

where S_b is a surface wrapped by the $SU(5)$ brane. The divisor η in S_b is related to a normal bundle $N_{S_b|\mathcal{B}}$ by the equation

$$c_1(N_{S_b|\mathcal{B}}) = 6K_{S_b} + \eta. \quad (4.39)$$

Finally λ is related to the G_4 flux and takes values in $\mathbb{Z} + \frac{1}{2}$ [45]. Note that the chirality formula (4.38) is a local expression on the surface S_b . In contrast, the chirality formula (2.1) is defined by integration over the whole resolved Calabi–Yau fourfold \tilde{X}_4 . In the current example, we chose $S_b = \mathbb{P}^2$ and $N_{S_b|\mathcal{B}} = \mathcal{O}_{\mathbb{P}^2}$. Hence, $\eta = 18H_{\mathbb{P}^2}$ where $H_{\mathbb{P}^2}$ is a hyperplane class of \mathbb{P}^2 . The chirality formula (4.38) becomes

$$n_{\mathbf{10}} = -\lambda(18H_{\mathbb{P}^1} \cdot_{\mathbb{P}^2} 3H_{\mathbb{P}^2}) = -54\lambda \quad (4.40)$$

One also finds the same number for the matter in the $\bar{\mathbf{5}}$ representation. Comparing the spectral cover result (4.40) with the result (4.30), we find agreement if we identify $3\beta = \lambda$. Since the chirality for the $\mathbf{10}$ matter fields and the chirality of $\bar{\mathbf{5}}$ matter fields are the same, the same identification is satisfied for the comparison between (4.40) and (4.30).

4.2 A $U(1)$ -restricted hypersurface with $SU(5) \times U(1)$ gauge group

In the previous subsection we have exemplified the use of the Mori cone generators and their connection to a non-Abelian gauge group $SU(5)$ on a single stack of 7-branes. We now present a second example where an additional geometrically massless $U(1)$ is present. In an $SU(5)$ model this $U(1)$ can be identified with the $U(1)_X$ in $SO(10)$. The geometric construction presented here corresponds to the $U(1)$ restricted Tate model introduced in [8].

The Calabi-Yau fourfold which we will construct has a base which is a \mathbb{P}^3 blown up along a curve into a surface S_b . The gauge group on S_b is engineered to be $SU(5)$. The points on edges of the polyhedron for the $U(1)_X$ restricted Tate model for such a setup

are:

points	divisor basis
-1 0 0 0 0	D_1
0 -1 0 0 0	D_2
3 2 0 0 0	$D_3 = \mathcal{B}$
3 2 1 1 1	$D_4 = H$
3 2 -1 0 0	D_5
3 2 0 -1 0	D_6
3 2 0 0 -1	D_7
3 2 1 1 0	$D_8 = \hat{S}$
2 1 1 1 0	$D_9 = B_1$
1 1 1 1 0	$D_{10} = B_2$
1 0 1 1 0	$D_{11} = B_3$
0 0 1 1 0	$D_{12} = B_4$
-1 -1 0 0 0	$D_{13} = X$

(4.41)

Note that the inclusion of the last vertex corresponding to $X = D_{13}$ enforces $a_6 = 0$ in the standard Tate constraint. Here a_6 is the coefficient of the z^6 term, with $z = 0$ being the base \mathcal{B} . This method can be quite generally applied to obtain a geometrically massless $U(1)$'s in the four-dimensional spectrum [8].

In (4.41) we have introduced the independent divisors $\mathcal{B}, H, \hat{S}, B_i$ and X . Note that B_1, \dots, B_4 are the exceptional divisors resolving the A_4 singularity. X originates from the resolution of an $SU(2)$ singularity along a curve outside S_b . As in (2.4) we introduce a divisor $S = \hat{S} + B_1 + B_2 + B_3 + B_4$. The Hodge numbers of the Calabi–Yau fourfold \tilde{X}_4 are

$$h^{1,1}(\tilde{X}_4) = 8, \quad h^{2,1}(\tilde{X}_4) = 0, \quad h^{3,1}(\tilde{X}_4) = 1020, \quad \chi(\tilde{X}_4) = 6216. \quad (4.42)$$

In the following we will determine the Mori vectors and follow the resolution process. This will allow us to determine the net chirality induced by an F-theory compatible flux.

4.2.1 Mori cone, resolutions and group theory

We begin our analysis with the determination of the Mori cone and its relation to the group theory of $SU(5) \times U(1)$. Restricting to star-triangulations of the polyhedron (4.41) including the origin, and using the method described in appendix B, we find twelve phases for the hypersurface. As in the previous example we use the star-triangulations ignoring the interior points in the facets. For simplicity we will focus on one phase in the following.

The generators of the Mori cone for the phase are

ℓ_1	ℓ_2	ℓ_3	ℓ_4	ℓ_5	ℓ_6	ℓ_7	ℓ_8
0	0	0	0	0	0	0	1
0	0	0	1	0	0	-1	1
-3	-1	1	0	0	0	0	0
0	1	0	0	0	0	0	0
1	0	0	0	0	0	0	0
1	0	0	0	0	0	0	0
0	1	0	0	0	0	0	0
1	-1	-2	0	0	1	0	0
0	0	1	0	1	-2	0	0
0	0	1	1	-1	0	0	0
0	0	0	-1	-1	1	1	0
0	0	0	0	1	0	-1	0
0	0	0	0	0	0	1	-1

(4.43)

The singular limit $\tilde{X}_4 \rightarrow X_4$ is the limit in which B_1, \dots, B_4 collapse to the surface S_b and X collapses to a curve. In this limit, each curve $\ell_4, \ell_5, \ell_6, \ell_7, \ell_8$ shrinks to a point in X_4 . Hence, they are the generators of the relative Mori cone. Note that the Cartan charges of $SU(5)$ are the same as the ones of (4.3). Furthermore, ℓ_3 intersects with the Cartan divisors. Hence, the generators of the extended relative Mori cone are $\ell_3, \ell_4, \ell_5, \ell_6, \ell_7, \ell_8$.

Some of the weights are charged under the new $U(1)$ which originates from the reduction along the Poincaré dual two-form of X . As for the Cartan divisor of the other $U(1)$, we use the divisor [8]

$$B_5 = X - B - [c_1(\mathcal{B})], \quad (4.44)$$

where $[c_1(\mathcal{B})] = H + D_5 + D_6 + D_7 + S$.⁸ This redefinition is required to ensure that the intersection numbers satisfy the vanishing condition (2.12) in this basis. The Poincaré dual two-form ω_5 of B_5 is used for the dimensional reduction to obtain the $U(1)_X$ gauge field A_X as $C_3 = A_X \wedge \omega_5$. From the intersection between B_i with $i = 1, \dots, 4$, and B_Λ with $\Lambda = 1, \dots, 5$, one obtains a part of the Cartan matrix of $SO(10)$ as [18]

$$B_i \cdot B_\Lambda \cdot D_\alpha \cdot D_\beta = \begin{pmatrix} -2 & 1 & 0 & 0 & 0 \\ 1 & -2 & 1 & 0 & 0 \\ 0 & 1 & -2 & 1 & 1 \\ 0 & 0 & 1 & -2 & 0 \end{pmatrix} \mathcal{B} \cdot S \cdot D_\alpha \cdot D_\beta. \quad (4.45)$$

Since $B_5 \cdot B_5$ does not localize on the surface S , the component C_{55} of (2.13) does not reproduce the 5 – 5 component of the $SO(10)$ Cartan matrix. This is consistent with a four-dimensional theory with gauge group $SU(5)_{GUT} \times U(1)_X$ rather than $SO(10)$, and matter representations originating from an underlying $SO(10)$. This precisely occurs in

⁸Here we use $[c_1(\mathcal{B})]$ including S instead of \hat{S} . More precisely, one could also write $\pi^*c_1(\mathcal{B})$. Any modification by a shift with blow-up divisors will just result in a change of basis in the following discussion.

the $U(1)_X$ restricted model as a global realization of the $(4+1)$ split spectral cover model considered in [9, 10]. Indeed, we can identify the weights corresponding to the generators of the Mori cone (4.43) with weights in the representation of $SO(10)$ when we identify the root corresponding to the Cartan divisor B_5 with $e_4 + e_5$ which is one of the simple roots of $SO(10)$.

Motivated by the intersections (4.45), we identify the Cartan divisors B_Λ , ($\Lambda = 1, \dots, 5$) with $e_1 - e_2, e_4 - e_5, e_2 - e_3, e_3 - e_4, e_4 + e_5$, which are the simple roots of $SO(10)$. From the Cartan charges in (4.43), one can also identify the curves $\ell_4, \ell_5, \ell_6, \ell_7, \ell_8$ with weights in the representation of $SO(10)$

$$\begin{aligned}
\ell_4 &\cong -\frac{1}{2}e_1 - \frac{1}{2}e_2 + \frac{1}{2}e_3 + \frac{1}{2}e_4 - \frac{1}{2}e_5 = +e_3 + e_4 - e_\Sigma, \\
\ell_5 &\cong \frac{1}{2}e_1 - \frac{1}{2}e_2 + \frac{1}{2}e_3 - \frac{1}{2}e_4 + \frac{1}{2}e_5 = -e_2 - e_4 + e_\Sigma, \\
\ell_6 &\cong -e_1 + e_2, \\
\ell_7 &\cong \frac{1}{2}e_1 + \frac{1}{2}e_2 - \frac{1}{2}e_3 + \frac{1}{2}e_4 + \frac{1}{2}e_5 = -e_3 + e_\Sigma, \\
\ell_8 &\cong -\frac{1}{2}e_1 - \frac{1}{2}e_2 - \frac{1}{2}e_3 - \frac{1}{2}e_4 - \frac{1}{2}e_5 = -e_\Sigma,
\end{aligned} \tag{4.46}$$

where e_Σ denotes $\frac{1}{2}(e_1 + e_2 + e_3 + e_4 + e_5)$. In terms of $SU(5)$, ℓ_4 corresponds to a weight in the **10** representation, ℓ_5 corresponds to a weight in the $\overline{\mathbf{10}}$ representation, and ℓ_7 corresponds to a weight in the $\overline{\mathbf{5}}$ representation. They are identical to the ones in the phase I of the first example (4.5). In the $U(1)_X$ restricted model, we can further understand their $SO(10)$ origins. The weights corresponding to ℓ_4 and ℓ_7 come from the **16'** representation and the weight corresponding to ℓ_5 comes from the **16** representation of $SO(10)$. We can also consider a weight corresponding to a curve $\ell_7 + \ell_8$

$$\ell_7 + \ell_8 \cong -e_3. \tag{4.47}$$

In $SU(5)$ this curve corresponds to a weight of the $\overline{\mathbf{5}}$ representation. Its $SO(10)$ origin is a weight of the **10** representation since $\pm e_a$ ($a = 1, \dots, 5$) are the weights of the **10** representation of $SO(10)$. Therefore, we have two types of $\overline{\mathbf{5}}$ representations originating from the **16'** and **10** representation of $SO(10)$. We also have a singlet field associated with the weight $-e_\Sigma$ which corresponds to the curve ℓ_8 . In addition, the generator ℓ_3 corresponds to the extended weight $e_1 - e_5$ up to a term e_Σ which is a singlet in $SU(5)$. This curve does not shrink in the singular limit and is an additional generator for the extended relative Mori cone.

From the relative Mori cone, one can determine the resolution structure. Since the $SU(5)$ Cartan charges of the $\ell_3, \ell_4, \ell_5, \ell_6, \ell_7$ are the same as the ones of the phase I in the first example (4.5), the resolution of the chains $A_4 \rightarrow D_5 \rightarrow E_6, D_6$ and $A_4 \rightarrow A_5 \rightarrow E_6, D_6$ are essentially the same except for the singlet term e_Σ . However, we have other chains $A_4 \rightarrow A_5 \rightarrow A_6$ and $A_4 \rightarrow A'_5 \rightarrow A_6$. The A_6 singularity enhancement appears as a point where the two A_5 and A'_5 singularity enhancement loci meet. Let us focus on the resolution along these chains. From the generators of the relative Mori cone, we have identified the two $\overline{\mathbf{5}}$ matter fields with ℓ_7 and $\ell_7 + \ell_8$. Therefore, the decompositions of the negative

simple roots along the two A_5 and A'_5 singularity enhancement loci are

$$-e_3 + e_4 = (-e_3 + e_\Sigma) + (e_4 - e_\Sigma), \quad (4.48)$$

$$-e_3 + e_4 = (-e_3) + (e_4). \quad (4.49)$$

Indeed, one can reconstruct the weights $e_4 - e_\Sigma$ and e_4 from the generators of the relative Mori cone

$$e_4 - e_\Sigma \cong \ell_4 + \ell_7 + \ell_8, \quad (4.50)$$

$$e_4 \cong \ell_4 + \ell_7 \quad (4.51)$$

Hence, both weights correspond to the effective curves in the relative Mori cone.

At the A_6 singularity enhancement points a further degeneration occurs in accord with the $SU(7)$ algebra. The $\mathbf{5}$ and $\bar{\mathbf{5}}$ weights arising from different $SO(10)$ representations are located at the A_6 points. From the decomposition (4.48), $-e_3 + e_\Sigma$ cannot further decompose into smaller pieces since it is already a generator of the relative Mori cone. However, $e_4 - e_\Sigma$ can decompose as

$$e_4 - e_\Sigma = (e_4) + (-e_\Sigma). \quad (4.52)$$

The consistent degeneration requires that (4.49) decomposes as

$$-e_3 = (-e_3 + e_\Sigma) + (-e_\Sigma), \quad (4.53)$$

and e_4 remains unchanged. We can see that the decompositions (4.52) and (4.53) also obey the $SU(7)$ algebra. To summarize, we have the curves corresponding to the weights

$$-e_1 + e_2, \quad -e_2 + e_3, \quad -e_3 + e_\Sigma, \quad -e_\Sigma, \quad e_4, \quad -e_4 + e_5, \quad (4.54)$$

at the A_6 singularity enhancement points. The degeneration chain is depicted in Figure 3.

4.2.2 G_4 -flux and chirality

In the $U(1)_X$ restricted model, we turn on a G_4 -flux of the following form⁹

$$G_4 = F_X \wedge \omega_{\tilde{X}}, \quad (4.55)$$

where $F_X = n^\alpha \omega_\alpha$, and $\omega_{\tilde{X}}$ is the Poincaré dual two-form to a linear combination of the exceptional divisors B_Λ , ($\Lambda = 1, \dots, 5$). This means that we turn on a gauge flux in the direction of $\omega_{\tilde{X}}$. Since we preserve the $SU(5)_{GUT}$ symmetry for all n^α , the condition (2.18), given by $\Theta_{i\beta} = 0$, reduces to

$$\int_{\tilde{X}_4} \omega_\alpha \wedge \omega_{\tilde{X}} \wedge \omega_i \wedge \omega_\beta = 0. \quad (4.56)$$

⁹In general, one can also include an additional flux $G_4 = m^{\Sigma\Lambda} \omega_\Sigma \wedge \omega_\Lambda$, we have checked that (2.18) restricts this Ansatz to a one-parameter family. In order to keep the analysis simple, we will not include this flux in the following.

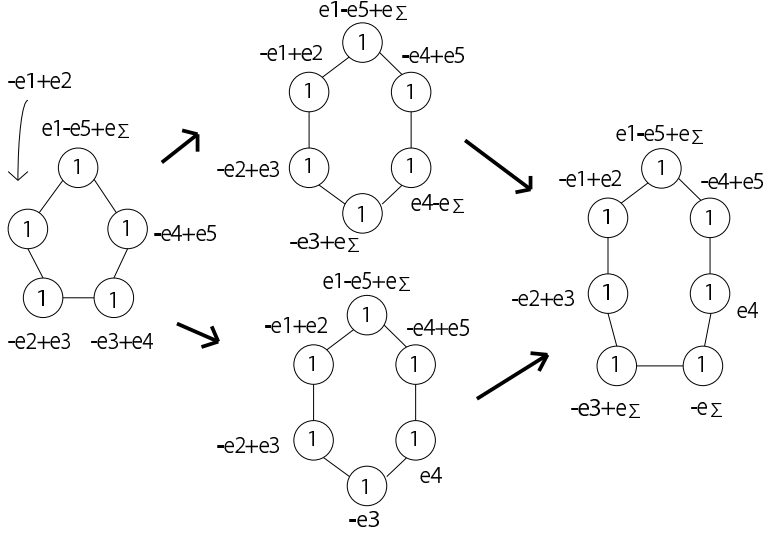


Figure 3: The chain of the Dynkin diagrams for $A_4 \rightarrow A_5 \rightarrow A_6$ and $A_4 \rightarrow A'_5 \rightarrow A_6$. e_Σ denotes the singlet weight $\frac{1}{2}(e_1 + e_2 + e_3 + e_4 + e_5)$. The number in the node denotes the multiplicity.

Then, $\omega_{\tilde{X}}$ can be determined up to an overall constant. The Poincaré dual to $\omega_{\tilde{X}}$ is

$$B_{\tilde{X}} = \alpha(-2B_1 - 4B_3 - 6B_4 - 3B_2 - 5B_5), \quad (4.57)$$

We later fix the overall constant α by requiring that the $U(1)$ direction $\omega_{\tilde{X}}$ matches the $U(1)_X$ considered in the (4+1) split spectral cover model. Furthermore, the G_4 -flux (4.55) should satisfy the condition (2.18). The condition can be satisfied when F_X is an element of $H^{1,1}(\mathcal{B})$ because of (2.12). Hence the Poincaré dual of F_X can be

$$F_X = aH + bS. \quad (4.58)$$

The first constraint of (2.18) is also satisfied due to the requirement (4.56).

Let us determine the charges for matter fields under the $U(1)_X$ obtained along (4.57). The Cartan charges can be computed by (3.6). We have seen in the previous subsection that the curve corresponding to the $\overline{\mathbf{10}}$ matter field is l_5 and the curves corresponding to the two $\mathbf{5}$ matter fields are l_7 and $l_7 + l_8$. One can determine their curve classes from the intersection numbers (4.43). Note that the curve classes in the Calabi–Yau fourfold can be expressed as the triple intersection of the divisors. When l_i has a negative intersection number with B_i , B_i can be chosen as a component in the triple intersection. Hence, we make the Ansätze

$$\begin{aligned} l_5 &= aB_2 \cdot B_3 \cdot (\mu H + \nu S), & l_7 &= \left(\sum_A a^A D_A \right) \cdot B_4 \cdot (\mu H + \nu S), \\ l_7 + l_8 &= \left(\sum_A b^A D_A \right) \cdot B_4 \cdot (\mu H + \nu S), & l_8 &= \left(\sum_A c^A D_A \right) \cdot X \cdot (\mu H + \nu S), \end{aligned} \quad (4.59)$$

where $\sum_A a^A D_A$ etc. are general linear combinations of the divisors in (4.41). The parameters a, a_A, b_A, c_A are determined from the intersection numbers (4.43). Then, the curve

classes for $\ell_5, \ell_7, \ell_7 + \ell_8$ and ℓ_8 are

$$\overline{\mathbf{10}} : \ell_5 \cong -e_2 - e_4 + e_\Sigma \rightarrow \frac{1}{3\mu-2\nu} B_2 \cdot B_3 \cdot (\mu H + \nu S), \quad (4.60)$$

$$\begin{aligned} \bar{\mathbf{5}} : \ell_7 \cong -e_3 + e_\Sigma &\rightarrow \frac{1}{(\mu-2\nu)(7\mu-2\nu)} \left(2\mu B_2 + (\mu+2\nu)B_3 \right. \\ &\quad \left. + (\mu+2\nu)B_4 - (\mu-2\nu)B_5 \right) \cdot B_4 \cdot (\mu H + \nu S), \end{aligned} \quad (4.61)$$

$$\begin{aligned} \bar{\mathbf{5}} : \ell_7 + \ell_8 \cong -e_3 &\rightarrow \frac{1}{4(\mu-2\nu)(3\mu-\nu)} (2(3\mu-2\nu)B_2 + (5\mu-2\nu)B_3 \\ &\quad + 2(3\mu-2\nu)B_4 + (\mu-2\nu)B_5) \cdot B_4 \cdot (\mu H + \nu S), \end{aligned} \quad (4.62)$$

$$\mathbf{1} : \ell_5 \cong -e_\Sigma \rightarrow \frac{1}{63\mu+94\nu} (6B_4 + 8H + B_5) \cdot X \cdot (\mu H + \nu S), \quad (4.63)$$

where we choose special representatives in the solutions just for simplicity. From the explicit forms (4.60)–(4.63), one can determine the charge under $U(1)_X$ for each weight

$$\ell_5 \rightarrow \overline{\mathbf{10}}_{-\alpha}, \quad \ell_7 \rightarrow \bar{\mathbf{5}}_{-3\alpha}, \quad \ell_7 + \ell_8 \rightarrow \bar{\mathbf{5}}_{2\alpha} \quad \ell_8 \rightarrow \mathbf{1}_{5\alpha}. \quad (4.64)$$

For the comparison to the $(4+1)$ split spectral cover model, we choose the direction of $U(1)$ from $\omega_{\tilde{X}}$ to be the $U(1)_X$ in the $(4+1)$ split spectral cover model. Hence, we take $\alpha = 1$ hereafter. Note that we have determined the matter representation curves directly from the generators of the extended relative Mori cone. This approach is different from the one discussed in [18]. In [18], the matter representation curves are determined from the direct computation of the degeneration of the Tate form as done in the appendix C by exploiting the Stanley-Reisner ideal.

The other information necessary for the computation of the chirality (2.1) are the matter surfaces $S_{\mathbf{10}}$ and $S_{\bar{\mathbf{5}}}$. They can be determined from the curves in the extended relative Mori cone. The curves are already obtained as (4.60)–(4.62). Then, we pull out $\mu H + \nu S$ with the correct multiplicity. The correct multiplicity can be computed from the consideration of the intersection between $\mu H + \nu S$ and the matter curve $\Sigma_{\mathbf{10}}, \Sigma_{\bar{\mathbf{5}}}$. The condition for the $\Sigma_{\mathbf{10}}$ matter curve is the same as (4.28). However, the $\Sigma_{\bar{\mathbf{5}}}$ curve splits into two components $a_{3,2} = w = 0$ and $a_1 a_{4,3} - a_{2,1} a_{3,2} = w = 0$, where $w = 0$ defines the surface S_b and the definitions of the $a_{i,j}$ can be found in (C.1), (C.2). The matter fields in the $\bar{\mathbf{5}}_{-3}$ and $\bar{\mathbf{5}}_2$ representation are localized along $a_{3,2} = w = 0$ and $a_1 a_{4,3} - a_{2,1} a_{3,2} = w = 0$, respectively. The matter fields in the singlet $\mathbf{1}_5$ are localized along the curve $a_{3,2} = a_{4,3} = 0$. Hence, the condition (3.28) becomes

$$\mathcal{B} \cdot S \cdot c_1(\mathcal{B}) \cdot (\mu H + \nu S) = 3\mu - 2\nu, \quad (4.65)$$

$$\mathcal{B} \cdot S \cdot (3c_1(\mathcal{B}) - 2c_1(N_{S|\mathcal{B}})) \cdot (\mu H + \nu S) = 7\mu - 2\nu, \quad (4.66)$$

$$\mathcal{B} \cdot S \cdot (5c_1(\mathcal{B}) - 3c_1(N_{S|\mathcal{B}})) \cdot (\mu H + \nu S) = 12\mu - 4\nu, \quad (4.67)$$

$$\mathcal{B} \cdot (3c_1(\mathcal{B}) - 2c_1(N_{S|\mathcal{B}})) \cdot (4c_1(\mathcal{B}) - 3c_1(N_{S|\mathcal{B}})) \cdot (\mu H + \nu S) = 63\mu + 94\nu. \quad (4.68)$$

Therefore, the matter surfaces are

$$S_{\overline{\mathbf{10}}_{-1}} = B_2 \cdot B_3, \quad (4.69)$$

$$S_{\overline{\mathbf{5}}_{-3}} = \frac{1}{\mu-2\nu}(2\mu B_2 + (\mu+2\nu)B_3 + (\mu+2\nu)B_4 - (\mu-2\nu)B_5) \cdot B_4, \quad (4.70)$$

$$S_{\overline{\mathbf{5}}_2} = \frac{1}{\mu-2\nu}(2(3\mu-2\nu)B_2 + (5\mu-2\nu)B_3 + 2(3\mu-2\nu)B_4 + (\mu-2\nu)B_5) \cdot B_4, \quad (4.71)$$

$$S_{\mathbf{1}_5} = (6B_4 + 8H + B_5) \cdot X. \quad (4.72)$$

With the G_4 flux (4.55) and the matter surfaces (4.69)–(4.72), we compute the chirality of the matter fields in each representation by using (2.1). The intersection between the matter surfaces (4.69)–(4.72) and the G_4 flux (4.55) yields the numbers

$$\begin{aligned} \chi(\overline{\mathbf{10}}_{-1}) &= \int_{S_{\overline{\mathbf{10}}_{-1}}} G_4 = -3a + 2b, & \chi(\overline{\mathbf{5}}_{-3}) &= \int_{S_{\overline{\mathbf{5}}_{-3}}} G_4 = -21a + 6b, \\ \chi(\overline{\mathbf{5}}_2) &= \int_{S_{\overline{\mathbf{5}}_2}} G_4 = 24a - 8b, & \chi(\mathbf{1}_5) &= \int_{S_{\mathbf{1}_5}} G_4 = 315a + 470b. \end{aligned} \quad (4.73)$$

Note that consistent with anomaly cancellation in the four-dimensional gauge theory one has $\chi(\mathbf{10}_1) = \chi(\overline{\mathbf{5}}_{-3}) + \chi(\overline{\mathbf{5}}_2)$.

It is important to stress that we did not address the quantization of the real scalars a, b defining the G_4 flux (4.55). In order to do that one has to evaluate the condition (2.16). It is a trivial task to compute $c_2(\tilde{X}_4)$ for a torically realized hypersurface. The complication lies in the question if the base elements chosen in (4.55) are actually part of a minimal integral basis of $H_{\mathbb{V}}^4(\tilde{X}_4, \mathbb{Z})$. Furthermore, (2.16) can imply that we have to switch on another component of G_4 to compensate for the half-integrality of $c_2(\tilde{X}_4)/2$.

4.2.3 Relation to three-dimensional Chern-Simons term

The chirality (4.73) can be obtained from the three-dimensional Chern-Simons term by using (2.26). Since the $SU(5)$ Cartan charges of the generators of the relative Mori cone for the $U(1)_X$ restricted model are the same as the ones in the first example, the effectiveness of the curves corresponding to the $\mathbf{10}$ weights and the $\overline{\mathbf{5}}$ weights are essentially the same. However, they are actually $\mathbf{16}$ representation or $\mathbf{10}$ representation of $SO(10)$ and the Cartan charge for the $U(1)$ obtained from B_5 is affected by the singlet term e_Σ . Hence, we also have to take into account the singlet term to compute the formula (2.26). Since the $\mathbf{10}$ weights of $SU(5)$ come from the $\mathbf{16}'$ weights of $SO(10)$, the weight $e_i + e_j$ is indeed the weight $e_i + e_j - e_\Sigma$. For the $\overline{\mathbf{5}}_{-3}$ weights coming from the $\mathbf{16}'$, the shift for the weight $-e_i$ is $-e_i + e_\Sigma$. The $\overline{\mathbf{5}}_2$ weight coming from the $\mathbf{10}$ weight of $SO(10)$ remains unchanged. These can be also seen explicitly by constructing the effective curves from the generators of the relative Mori cone. Then, all the $U(1)$ charges for B_Λ , ($\Lambda = 1, \dots, 5$) can be obtained

from the weights of $SO(10)$ and the formula (2.26) becomes

$$\begin{aligned}
\Theta_{23} &= -\chi(\mathbf{10}), & \Theta_{24} &= \frac{1}{2}\chi(\mathbf{10}) + \frac{1}{2}(\chi(\bar{\mathbf{5}}_{-3}) + \chi(\bar{\mathbf{5}}_2)), \\
\Theta_{33} &= \chi(\bar{\mathbf{5}}_{-3}) + \chi(\bar{\mathbf{5}}_2), & \Theta_{44} &= -\chi(\mathbf{10}), \\
\Theta_{45} &= \frac{1}{2}\chi(\mathbf{10}) - \frac{1}{2}\chi(\bar{\mathbf{5}}_{-3}) + \frac{1}{2}\chi(\bar{\mathbf{5}}_2), & \Theta_{55} &= -\chi(\mathbf{10}) + \frac{3}{2}\chi(\bar{\mathbf{5}}_{-3}) - \chi(\bar{\mathbf{5}}_2) + \frac{1}{2}\chi(\mathbf{15}), \\
\Theta_{13} &= \frac{1}{2}\chi(\mathbf{10}) - \frac{1}{2}(\chi(\bar{\mathbf{5}}_{-3}) + \chi(\bar{\mathbf{5}}_2)), & \Theta_{34} &= \frac{1}{2}\chi(\mathbf{10}) - \frac{1}{2}(\chi(\bar{\mathbf{5}}_{-3}) + \chi(\bar{\mathbf{5}}_2)), \\
\Theta_{11} &= -\chi(\mathbf{10}) + \chi(\bar{\mathbf{5}}_{-3}) + \chi(\bar{\mathbf{5}}_2), & \Theta_{22} &= \chi(\mathbf{10}) - (\chi(\bar{\mathbf{5}}_{-3}) + \chi(\bar{\mathbf{5}}_2)), \tag{4.74}
\end{aligned}$$

and the other components are zero. From the explicit intersection numbers by using the G_4 -flux (4.55), $\Theta_{\Lambda\Sigma}$ is computed to be

$$\begin{aligned}
\Theta_{23} &= -3a + 2b, & \Theta_{24} &= 3a - 2b, & \Theta_{33} &= 3a - 2b, & \tag{4.75} \\
\Theta_{44} &= -3a + 2b, & \Theta_{45} &= 24a - 8b, & \Theta_{55} &= 99a + 254b,
\end{aligned}$$

and the other components are zero. The chirality of (4.73) is precisely reproduced by comparing (4.74) with the explicit expressions (4.75).

4.2.4 Comparison with split spectral cover

Having obtained the chirality (4.73) from the formula (2.1), we compare the results with the ones from the $(4+1)$ split spectral cover model.

As for the $U(1)_X \in SU(5)_\perp$, we consider the generator $(1, 1, 1, 1, -4) \in SU(5)_\perp$. Then, we have the matter fields localized on the GUT surface S_b

$$\mathbf{10}_1, \quad \bar{\mathbf{5}}_{-3}, \quad \bar{\mathbf{5}}_2, \tag{4.76}$$

where subscript denotes the charge under the $U(1)_X$. The $\bar{\mathbf{5}}_{-3}$ representation matter fields are localized along $a_{3,2} = w = 0$ and the $\bar{\mathbf{5}}_2$ matter fields are localized along $a_1 a_{4,3} - a_{2,1} a_{3,2} = w = 0$. The chirality formulas for $\mathbf{10}$ and $\bar{\mathbf{5}}$ matter are [9, 10]

$$\chi_{\mathbf{10}} = (-\lambda\tilde{\eta} + \frac{1}{4}\zeta) \cdot (\tilde{\eta} - 4c_1(S_b)), \tag{4.77}$$

$$\chi_{\bar{\mathbf{5}}_{-3}} = \lambda(-\tilde{\eta}^2 + 6\tilde{\eta}c_1(S_b) - 8c_1^2(S_b)) + \frac{1}{4}\zeta(-3\tilde{\eta} + 6c_1(S_b)), \tag{4.78}$$

$$\chi_{\bar{\mathbf{5}}_2} = \lambda(-2\tilde{\eta}c_1(S_b) + 8c_1^2(S_b)) + \frac{1}{4}\zeta(4\tilde{\eta} - 10c_1(S_b)), \tag{4.79}$$

where $\tilde{\eta} = \eta - c_1(S_b)$ and η is related to the first Chern class of the normal bundle (4.39). ζ is a flux part on S , namely $\zeta \in H^2(S_b, \mathbb{Z})$. In the current example (4.41), ζ can be chosen as

$$\frac{1}{4}\zeta = (aH + bS)|_{S_b}. \tag{4.80}$$

Then, the chirality formulas (4.77)–(4.79) can be computed as

$$\chi_{\mathbf{10}} = 3a - 2b - 38\lambda, \quad \chi_{\bar{\mathbf{5}}_{-3}} = -21a + 6b - 22\lambda, \quad \chi_{\bar{\mathbf{5}}_2} = 24a - 8b - 16\lambda. \tag{4.81}$$

For the comparison with the results of (4.73) note that we turn on the G_4 flux only in the direction of the $U(1)_X$ (4.55). This corresponds to the case where $\lambda = 0$ in the $(4+1)$ split spectral cover model. By putting $\lambda = 0$, (4.81) exactly reproduce the chirality formulas (4.73) when we identify $\frac{1}{4}\zeta$ with F_X .

5. Conclusions

In this paper we discussed the determination of the net chiral matter spectrum of a four-dimensional F-theory compactification on a singular Calabi-Yau manifold X_4 . We argued that the description of F-theory as a limit of M-theory allows to extract these data on the resolved fourfold \tilde{X}_4 with G_4 flux. The resolution is physical in the effective three-dimensional theory obtained from M-theory on \tilde{X}_4 , and corresponds to moving to the Coulomb branch of the gauge theory. Due to the G_4 fluxes the resulting theory contains Chern-Simons couplings, proportional to $\Theta_{\Lambda\Sigma} A^\Lambda \wedge F^\Sigma$, for the $U(1)$ vector fields A^Λ . In contrast, such couplings are not induced by a classical circle reduction of a general four-dimensional $\mathcal{N} = 1$ theory which arises as the low energy limit of F-theory on X_4 . However, upon reduction to three dimensions the charged matter becomes massive in the Coulomb branch of the gauge theory. This precisely corresponds to the resolution process of X_4 to \tilde{X}_4 . The Chern-Simons couplings are then induced by one-loop corrections with the massive charged matter running in the loop. Matching the Chern-Simons couplings of the fluxed M-theory reduction with the one-loop corrections in the F-theory reduction, we argued that the map between G_4 fluxes and net chiral matter can be inferred.

The study of one-loop corrections in the three-dimensional Chern-Simons theory requires the knowledge of the $U(1)$ charges, as well as some positivity properties of the scalars in the three-dimensional vector multiplets. Geometrically this corresponds to the fact that curves associated to the singularity resolution can have positive or formally negative volume. This led us to introduce the relative Mori cone which contains all effective curves of \tilde{X}_4 which shrink to points in X_4 . A detailed map between these curves and the weights of different representations of the matter fields allowed a deeper understanding of the resolution process at co-dimensions two and three where matter and Yukawa couplings are localized. With this data at hand the one-loop Chern-Simons couplings can be evaluated and matched with the G_4 flux result $\Theta_{\Lambda\Sigma}$. The expressions manifestly depend on the number of charged fermions and led to a computation of the chiral index $\chi(\mathbf{R})$. While we have shown this for single non-Abelian gauge groups quite generally, it would be interesting to find a more group-theoretic reasoning that the index $\chi(\mathbf{R})$ can always be extracted.

An analysis of the extended relative Mori cone using the \tilde{X}_4 -intersection numbers resulted in a detailed map between weights and resolution curves. We then proposed a formalism to determine the matter surfaces $S_{\mathbf{R}}$ which extract the chiral index directly from viable G_4 -fluxes via $\chi(\mathbf{R}) = \int_{S_{\mathbf{R}}} G_4$. We have shown that $S_{\mathbf{R}}$ can be constructed for a chosen weight of the representation \mathbf{R} . Only the integral $\chi(\mathbf{R})$ is independent of the weight and the topological phase of the resolution. From the Chern-Simons analysis one realizes that $\chi(\mathbf{R})$ can be written as $\chi(\mathbf{R}) = t_{\mathbf{R}}^{\Lambda\Sigma} \Theta_{\Lambda\Sigma}$, where $t_{\mathbf{R}}^{\Lambda\Sigma}$ is either determined from the matter surface, or from the charges and positivity properties of the curve classes. It would be nice to work out more details of the map from the resolution geometry to $t_{\mathbf{R}}^{\Lambda\Sigma}$.

In the last part of the paper we have evaluated the net chirality for two specific examples with $SU(5)$ and $SU(5) \times U(1)_X$ gauge group. We have found that in the first example there is a single parameter encoding G_4 flux which preserves four-dimensional Poincaré invariance

and does not break the $SU(5)$ gauge symmetry. This is consistent with a spectral cover construction. However, our construction does not depend on the existence of a globally valid spectral cover description. In the second example we only included the $U(1)$ -flux gauging the $U(1)_X$, and determined the induced net chirality. The result was successfully matched with the split spectral cover construction for states localized on the $SU(5)$ brane. The number of singlets localized away from the $SU(5)$ -brane can equally be determined using our construction. Both the Chern-Simons analysis as well as the explicit construction of the matter surfaces led to matching answers. It would be interesting to generalize the flux in this configuration. It can indeed be checked that there exists a one-parameter family of G_4 fluxes which do break $SU(5)$ and induce new chiral fields. Matching with a global split spectral cover is hard in this case, since this universal flux is not entirely localized on the $SU(5)$ -brane, and our model has no heterotic dual. So while it is straightforward to evaluate the chirality using our formalism, there are not many results with which we can compare the answer. One other issue, which we addressed only briefly, is to determine the correct quantization conditions on the parameters determining the flux G_4 . It is straightforward to compute the second Chern class for our examples which is required to evaluate (2.16). The complication lies in the determination of a minimal integral basis of $H^4(\tilde{X}_4, \mathbb{Z})$. It would be interesting to do that for both the $SU(5)$ and $SU(5) \times U(1)_X$ model, e.g. by using the explicit hypersurface equation and resolution. One expects also an interpretation of these quantization conditions in the three-dimensional Chern-Simons theory.

An interesting extension of this work would be the systematic study of more complicated examples with varying gauge groups and representations. This includes cases with multiple non-Abelian factors, to which our formalism has to be extended. Furthermore, already the exceptional gauge group cases might yield some interesting new properties which can be studied for a given \tilde{X}_4 . Much of our formalism can be algorithmically implemented in a computer search. One of the main challenges will remain the systematic implementation of the quantization conditions.

Acknowledgments: We would like to thank Federico Bonetti, Iñaki García-Etxebarria, Kenji Hashimoto, Denis Klevers, Albrecht Klemm, Seung-Joo Lee, Noppadol Mekareeya, Raffaele Savelli, Gary Shiu, Wati Taylor, and Timo Weigand for discussions. HH would like to thank the Hong Kong Institute for Advanced Study at HKUST and Max-Planck-Institut für Physik for hospitality and financial support during part of this work. The work of TG was supported by a research grant of the Max Planck Society. The work of HH research was supported in part by JSPS Research Fellowships for Young Scientists.

Appendices

A. Six-dimensional matter via five-dimensional loops

In this appendix we describe how the 6d F-theory spectrum can be extracted from a 5d compactification of M-theory on a resolved Calabi-Yau threefold. Six-dimensional F-theory compactifications have been reviewed in detail in [46].¹⁰ A more complete analysis of the 6d effective action and the analysis of the spectrum using loop corrections of 5d Chern-Simons theory can be found in [30]. If this is done for a resolved threefold \tilde{X}_3 the resulting 5d $\mathcal{N} = 2$ theory will be in its Coulomb branch. In the effective theory one will find a Chern-Simons coupling of the form

$$S_{\text{CS}}^{(5)} = \int_{\mathbb{M}^{4,1}} \mathcal{K}_{ABC} A^A \wedge F^B \wedge F^C \quad (\text{A.1})$$

where A^A are the 5d vectors which arise by expanding the M-theory three-form into a basis of $(1,1)$ -forms of X_3 . The coefficients \mathcal{K}_{ABC} in (A.1) are precisely the intersection numbers of \tilde{X}_3 . One realizes that upon lifting these couplings to an F-theory compactification to six dimensions, terms coupling with \mathcal{K}_{ijk} , i.e. the intersections of the exceptional divisors for the resolved singularities, are absent at in the tree-level effective action. In fact, it is known that these couplings precisely arise from a one loop correction to the 5d gauge theory with Coulomb-branch $U(1)$'s A^i . On the gauge theory side these corrections can also be determined in terms of the number of hypermultiplets in various representations which became massive when going to the Coulomb branch. In other words, in the 5d theory one precisely finds the link of the intersection numbers \mathcal{K}_{ijk} with the charged matter spectrum.

Five dimensional gauge theories with matter fields have a prepotential of the form [25]

$$\mathcal{F} = \frac{1}{2} m_0 h_{ij} \xi^i \xi^j + \frac{1}{6} c_{\text{class}} d_{ijk} \xi^i \xi^j \xi^k + \frac{1}{12} \left(\sum_{\mathbf{R}} |\mathbf{R} \cdot \xi|^3 - \sum_f \sum_{\mathbf{w} \in \mathbf{W}_f} |\mathbf{w} \cdot \xi + m_f|^3 \right), \quad (\text{A.2})$$

where $h_{ij} = \text{Tr}(T_i T_j)$ and $d_{ijk} = \frac{1}{2} \text{Tr} T_i (T_j T_k + T_k T_j)$ with T_i the Cartan generator of a gauge group G . \mathbf{R} are the roots of G , \mathbf{W}_f are the weights of G in the representation of \mathbf{r}_f . The first two terms of (A.2) are the classical terms and the last two terms of (A.2) are the quantum contributions of massive charged vector and matter multiplets. ξ_i is a real scalar field in a vector multiplet. Geometrically, ξ_i comes from the dimensional reduction of Kähler forms which are Poincaré dual to exceptional divisors $\tilde{J} = \xi^i \omega_i$. It is not hard to compare the field theoretic expression (A.2) with the pre-potential $\mathcal{F}(\xi^i) = \frac{1}{6} \mathcal{K}_{ijk} \xi^i \xi^j \xi^k$ arising in the M-theory compactification, and derive the identification of the coefficients \mathcal{K}_{ijk} with the number of charged matter fields in the various representations.

Let us now see more explicitly how the matter content in five dimensional $SU(N)$ gauge theories is determined from the triple intersection numbers of the exceptional divisors. The

¹⁰An incomplete list of recent works on this subject includes [47, 48, 49].

prepotential (A.2) for $SU(N)$ gauge theories can be written as

$$\frac{1}{6}\mathcal{K}_{ijk}\xi^i\xi^j\xi^k = \frac{1}{12}\left((2-2n_{\mathbf{Adj}})\sum_{I<J}^N(a^I-a^J)^3+2c_{\text{class}}\sum_{I=1}^N(a^I)^3-n_{\mathbf{AS}}\sum_{I<J}^N|a^I+a^J|^3-n_{\mathbf{F}}\sum_{I=1}^N|a^I|^3\right), \quad (\text{A.3})$$

where a^I 's are vevs of a vector multiplet $\Phi = \text{diag}(a^1, \dots, a^N)$ and parameterize the Coulomb branch. Here we include the contribution from matter in the adjoint representation, the fundamental representation and the anti-symmetric representation. We suppress the contribution from the symmetric representation fields since their contribution is the same as the one from an anti-symmetric tensor and eight fundamentals. Note that to compare this term with the expression obtained by the Calabi-Yau reduction of M-theory one has to identify the $a^I, I = 1 \dots N$ with the $N - 1$ expansion coefficients of the rescaled Kähler form $J = \xi^i \omega_i$ as

$$a^1 = \xi^1, \quad a^N = -\xi^{N-1}, \quad (\text{A.4})$$

$$a^I = \xi^I - \xi^{I-1}, \quad I = 2, \dots, N - 1 \quad (\text{A.5})$$

We can write general expressions for the matter content of the fundamental representation matter and anti-symmetric representation matter in $SU(N)$ gauge theories in terms of the triple intersection numbers by exploiting the relation (A.3). The formulas in the case of $n_{\mathbf{AS}} = 0$ was obtained in [25] purely from geometry. We propose the generalization of the results including anti-symmetric representation matter assuming (A.3). We also assume that there are only fields in the adjoint representation, the fundamental representation and anti-symmetric representation. We propose the generalized formulas are

$$D_j^2 D_{j+1} + D_j D_{j+1}^2 = 2n_{\mathbf{Adj}} - 2, \quad (\text{A.6})$$

$$D_j^3 = 8 - 8n_{\mathbf{Adj}} - an_{\mathbf{AS}} - bn_{\mathbf{F}}, \quad (\text{A.7})$$

$$D_i D_j D_k = 0 \text{ or } n_{\mathbf{AS}}, \quad (\text{A.8})$$

where i, j, k in (A.8) are all different. The coefficient of a and b in (A.7) can be determined in the following way. The parameters of the Coulomb branch, namely $\mathbf{w}_{\mathbf{f}} \cdot \xi = a^I$ for a fundamental representation weight $\mathbf{w}_{\mathbf{f}}$ and $\mathbf{w}_{\mathbf{as}} \cdot \xi = a^I + a^J$ for an anti-symmetric representation weight $\mathbf{w}_{\mathbf{as}}$, are positive or negative depending on the sub-wedge of the Weyl chamber in the Coulomb branch. For each phase, there are some weights whose signs change after one subtracts a simple root from them. Then, a and b are determined by counting how many simple roots α_j corresponding to D_j have such a feature.

For example, let us consider the relative Mori cone for the phase I in (4.3).¹¹ In this phase, a^1, a^2 are positive and a^3, a^4, a^5 are negative. Then, we have the relation

$$e_2 \cdot \xi - (e_2 - e_3) \cdot \xi = e_3 \cdot \xi. \quad (\text{A.9})$$

¹¹Although the relative Mori cone for the phase I was determined from the Calabi-Yau fourfolds (4.1), one can also obtain the same relative Mori cone for a Calabi-Yau threefold with a similar singularity structure.

Hence, $b = 1$ for D_2^3 where D_2 corresponds to a simple roots $e_2 - e_3$ and $b = 0$ for the other D_j^3 's. For the $\mathbf{10}$ weights, the sign for the Coulomb branch parameters are depicted in Figure 1. The sign change happens from $a^2 + a^4$ to $a^3 + a^4$ and from $a^2 + a^5$ to $a^3 + a^5$. Then, we have the relations

$$(e_2 + e_4) \cdot \xi - (e_2 - e_3) \cdot \xi = (e_3 + e_4) \cdot \xi, \quad (\text{A.10})$$

$$(e_2 + e_5) \cdot \xi - (e_2 - e_3) \cdot \xi = (e_3 + e_5) \cdot \xi. \quad (\text{A.11})$$

Hence, $a = 2$ for D_2^3 and $a = 0$ for the other D_j^3 's. Schematically, a and b for the triple intersection D_j^3 are written as

$$a = \#(e_j - e_{j+1}) \text{ s.t. } \mathbf{w}_{\mathbf{as}}(+)- (e_j - e_{j+1}) = \mathbf{w}_{\mathbf{as}}(-), \quad (\text{A.12})$$

$$b = \#(e_j - e_{j+1}) \text{ s.t. } \mathbf{w}_{\mathbf{f}}(+)- (e_j - e_{j+1}) = \mathbf{w}_{\mathbf{f}}(-) \quad (\text{A.13})$$

for each phase. Note that the formulas (A.6)–(A.8) are enough to determine the three unknown parameters $n_{\mathbf{Adj}}$, $n_{\mathbf{AS}}$ and $n_{\mathbf{F}}$. We have checked that the proposed formulae (A.6)–(A.8) correctly reproduce the relation (A.3) at least for $SU(5)$, $SU(6)$ and $SU(7)$ gauge theories.

For completeness, we review how to obtain the matter spectrum in six-dimensional theories from F-theory compactifications. The matter content of six-dimensional theories are constrained from the anomaly cancellation conditions [50]. The anomaly cancellation via Green-Schwarz mechanism [51, 52] requires that the anomaly eight-form should be factorized in a particular way. F-theory compactifications require that Calabi–Yau threefolds X_3 have an elliptic-fibration over the surface \mathcal{B}_2 . Then, the matter content from F-theory compactifications on X_3 is [50]

$$\text{index}(\mathbf{Ad}_a) - \sum_{\mathbf{r}} \text{index}(\mathbf{r}_a) n_{\mathbf{r}_a} = 6(K_{\mathcal{B}_2} \cdot D_a), \quad (\text{A.14})$$

$$y_{\mathbf{Ad}_a} - \sum_{\mathbf{r}} y_{\mathbf{r}_a} n_{\mathbf{r}_a} = -3(D_a \cdot D_a), \quad (\text{A.15})$$

$$x_{\mathbf{Ad}_a} - \sum_{\mathbf{r}} x_{\mathbf{r}_a} n_{\mathbf{r}_a} = 0, \quad (\text{A.16})$$

$$\sum_{\mathbf{r}, \mathbf{r}'} \text{index}(\mathbf{r}_a) \text{index}(\mathbf{r}'_b) n_{\mathbf{r}_a \mathbf{r}_b} = (D_a \cdot D_b), \quad (\text{A.17})$$

where D_a is a curve where a 7-brane wraps on. The matter in the representations \mathbf{Ad}_a , \mathbf{r}_a are localized on the 7-brane wrapping on the curve D_a . $x_{\mathbf{r}_a}, y_{\mathbf{r}_a}$ are defined as the coefficients in the decomposition

$$\text{tr}_{\mathbf{r}_a} F^4 = x_{\mathbf{r}_a} \text{tr} F^4 + y_{\mathbf{r}_a} (\text{tr} F^2)^2, \quad (\text{A.18})$$

Here we assume that \mathbf{r}_a has two independent fourth order invariants. If \mathbf{r}_a has only one fourth order invariant, then $x_{\mathbf{r}_a} = 0$. Let us see the formulas (A.14)–(A.17) more explicitly for an $SU(N)$ case. The coefficients in (A.18) are

$$\text{tr}_{\mathbf{Adj}} F^4 = 2N \text{tr} F^4 + 6 \text{tr} (F^2)^2, \quad (\text{A.19})$$

$$\text{tr}_{\mathbf{AS}} F^4 = (N - 8) \text{tr} F^4 + 3 (\text{tr} F^2)^2, \quad (\text{A.20})$$

for the $SU(N)$ case. The index of each representation is

$$\text{index}(\mathbf{F}) = 1, \quad \text{index}(\mathbf{AS}) = N - 2, \quad \text{index}(\mathbf{Adj}) = 2N. \quad (\text{A.21})$$

Inserting (A.19)–(A.21) into (A.14)–(A.16), we find

$$n_{\text{Adj}} = g, \quad n_{\mathbf{AS}} = -(K \cdot D), \quad n_{\mathbf{F}} = -8(K_{\mathcal{B}_2} \cdot D) - N(D \cdot D), \quad (\text{A.22})$$

where g is a genus of the curve D on which the $SU(N)$ 7-branes wrap.

The formulas (A.14)–(A.17) determine the spectrum for charged matter fields in six-dimensional theories from F-theory compactifications. They are written by the local geometric data on the base \mathcal{B}_2 . On the other hand, the matter content of five-dimensional gauge theories are characterized by the intersection between the exceptional divisors of resolved Calabi–Yau threefolds \tilde{X}_3 . Both spectrum should be the same due to the duality between M-theory and F-theory. For $SU(N)$ gauge theories, the spectrum obtaining from the formulas (A.6)–(A.8) from five-dimensional theories should match the spectrum from the six-dimensional theories formulas (A.22). Indeed, we have explicitly checked the exact matching of the charged matter spectrum in several examples of $SU(5)$ gauge theories.

B. Mori cone of hypersurfaces in toric varieties

We review how to obtain the generators of the Mori cone systematically by following the algorithm presented in [39, 40, 41]. We consider a hypersurface in a ambient toric space. Note that this algorithm can be also applied to complete intersections in principle. Let the polar polyhedron of the ambient toric space be Δ^* which is d dimension. For example, $d = 5$ for Calabi–Yau fourfold hypersurfaces. We denote the vertices of Δ^* by $\nu^{*(i)}$, where i labels the vertices. The origin of Δ^* is chosen to be $\nu^{*(0)}$. We first derive the generators of the Mori cone for the ambient toric space Δ^* . Then, we have to specify a particular star triangulation. This means that we subdivides Δ^* into a set of d dimensional simplices where every simplex includes the vertex $\nu^{*(0)}$. This triangulation procedure is not unique. We have in general many triangulations from one Δ^* , namely we have different Calabi–Yau hypersurfaces from the triangulation.

Let us pick one of the star triangulations. The generators of the Mori cone for this particular star triangulation of the ambient toric space Δ^* can be obtained systematically in the following way [39]:

1. Extend the vertices $\nu^{*(i)}$ to $\bar{\nu}^{*(i)} = (1, \nu^{*(i)})$.
2. Take all the pairs of the d dimensional simplices (S_k, S_l) which share a $(d - 1)$ dimensional simplex
3. For each pair, find a linear relation $\sum_i \ell_i^{k,l} \bar{\nu}^{*(i)} = 0$ among the vertices of $S_k \cup S_l$. Furthermore, the coefficients $\ell_i^{k,l}$ should be minimal integers and the coefficients of the points $(S_k \cup S_l) \setminus (S_k \cap S_l)$ should be non-negative.

4. Find a set of generators ℓ_i which express any $\ell_i^{k,l}$ of all the phases by the linear combination of the elements in the set with positive integer coefficients. The generators ℓ_i are the generators of the Mori cone of Δ^* of a particular phase.

So far we have determined the generators of the Mori cone for the toric ambient space Δ^* . Let us next turn to the generators of the Mori cone of Calabi–Yau hypersurfaces in the ambient space. In general, the Mori cone of an ambient space is different from the Mori cone of a hypersurface in the ambient space. In order to see how the Mori cone changes for hypersurfaces, let us see how the Kähler cone, which is dual to the Mori cone, changes for hypersurfaces first. The different Kähler cones from the different triangulations of the ambient space are connected through the boundaries of the Kähler cone. They are related to each other by flop transitions. Let us focus on one of the walls of the Kähler cone of the ambient space. When one passes the wall of the Kähler cone, a submanifold of the ambient space in one phase blows down on one side and another submanifold of the ambient space in another phase emerges on the other side of the wall. By restricting to the hypersurface in the ambient space, the submanifold which is flopped may not be contained in the hypersurface. In that case, the wall describing the flop of the ambient space is not a part of the Kähler cone of the hypersurface. Hence, we have to connect the two Kähler cones of the ambient space. By checking all the walls of the Kähler cones of the ambient space and removing the walls which are not related to the flops in the hypersurface, one can obtain the enlarged Kähler cone of the hypersurface. The dual to the union of the Kähler cones is the intersection of the corresponding Mori cones. Therefore, we consider the intersection of the Mori cones which characterizes one phase for the hypersurface in the ambient space.

For the ambient toric space, this procedure can also be computed systematically by exploiting the Stanley-Reisner ideal of the ambient toric space [40]:

1. Find all pairs of the triangulations which are related to each other by a flop through the co-dimension one boundary of the Kähler cones.
2. For each pair, pick up a generator of the Mori cone which blows down/up through the wall.
3. Determine a submanifold which contains the curve from the negative intersection numbers. The submanifold can be written by the intersection of the divisors of the ambient toric space.
4. Restrict a Calabi–Yau hypersurface equation on the intersection of the divisors.
5. If the hypersurface equation reduces to a monomial and the reduced defining equation is not compatible with the Stanley-Reisner ideal, then the flop does not exist in the hypersurface. If not, the flop exists in the hypersurface.
6. Try the procedures 3 ~ 5 for all the pairs.

7. Take the intersection of the Mori cones which are related by the flops which do not exist in the hypersurface. The generators of the intersection of the Mori cones are the generators of the Mori cone of the hypersurface.

Note that we only use the information of the hypersurface for writing down its defining equation. Since we can also write down the defining equation of complete intersections in the ambient toric variety, we can in principle apply this procedure to complete intersection Calabi–Yau manifolds.

Actually, there is a shortcut for the above procedures. Since the different phases of Calabi–Yau hypersurfaces have distinct intersection numbers, one can find a set of Mori cones which describes one phase of the hypersurface. The intersection numbers of hypersurfaces can be computed by restricting the ambient space divisors to the hypersurface. If all intersection numbers of the hypersurface are equal for some phases of the ambient toric space, they are actually a single phase of the hypersurface. Therefore, we can obtain the Mori cone for the hypersurface from the intersection of the Mori cones which generate the same intersection numbers on the hypersurface.

C. Resolution from Tate form

In the section 4.1.1, we have determined the degeneration of the \tilde{X}_4 -fibers from the Mori cone of the Calabi–Yau fourfold (4.1). In this appendix, we describe the degeneration from the direct analysis of the defining equation. The procedure applied here essentially follows [18] but for the case $a_6 \neq 0$. The defining equation of the elliptically fibered Calabi–Yau fourfold can be written by the Tate form

$$P = \{y^2 + a_1xyz + a_3yz^3 = x^3 + a_2x^2z^2 + a_4xz^4 + a_6z^6\}. \quad (\text{C.1})$$

For the Calabi–Yau fourfold X_4 , the divisors $D_{1,2,3}$ corresponds to $y = 0, x = 0, z = 0$ respectively.¹² If one imposes the A_4 singularity along the $w = 0$, then the coefficients of (C.1) have to take special forms

$$a_1 = a_1, \quad a_2 = a_{2,1}w, \quad a_3 = a_{3,2}w^2, \quad a_4 = a_{4,3}w^3, \quad a_6 = a_{6,5}w^5. \quad (\text{C.2})$$

In our example, $w = 0$ is the divisor D_4 . Introducing the divisors D_9, \dots, D_{12} resolve the A_4 singularity. The resolution process is

$$(x, y, w) \rightarrow (\tilde{x}E_1, \tilde{y}E_1, \tilde{w}E_1), \quad (\text{C.3})$$

$$y \rightarrow y_1w \quad (x, y_1, w) \rightarrow (\tilde{x}E_4, \tilde{y}_1E_4, \tilde{w}E_4), \quad (\text{C.4})$$

$$x \rightarrow x_1w \quad (x_1, y_1, w) \rightarrow (\tilde{x}_1E_2, \tilde{y}_1E_2, \tilde{w}E_2), \quad (\text{C.5})$$

$$y_1 \rightarrow y_2w \quad (x_1, y_1, w) \rightarrow (\tilde{x}_1E_3, \tilde{y}_2E_3, \tilde{w}E_3), \quad (\text{C.6})$$

¹²To be precise, $D_{1,2,3}$ are the divisors defined by the coordinates after the resolution.

where $E_1 = 0, E_2 = 0, E_3 = 0, E_4 = 0$ denote the divisors $D_9, D_{11}, D_{12}, D_{10}$ respectively. Note that for each line, we omit tilde when one moves on to the next line. Hence the resolution can be summarized as

$$(x, y, w) \rightarrow (\tilde{x}E_1E_2^2E_3^2E_4, \tilde{y}E_1E_2^2E_3^3E_4^2, \tilde{w}E_1E_2E_3E_4). \quad (\text{C.7})$$

By the resolution (C.7), the proper transform of the defining equation (C.1) of the Calabi–Yau fourfold becomes

$$\begin{aligned} \tilde{P} = \{ & y^2E_3E_4 + a_1xyz + a_{3,2}yz^3E_0^2E_1E_4 = x^3E_1E_2^2E_3 + a_{2,1}x^2z^2E_0E_1E_2 \\ & + a_{4,3}xz^4E_0^3E_1^2E_2E_4 + a_{6,5}z^6E_0^5E_1^3E_2E_4^2 \}. \end{aligned} \quad (\text{C.8})$$

where we rewrite $w \rightarrow E_0$ since the $E_0 = 0$ divisor correspond to a extended node of the extended A_4 Dynkin diagram.

The curve corresponding to the negative simple roots of the $SU(5)$ can be described by the intersection

$$\begin{aligned} e_1 - e_5 &= \hat{S} \cdot D_\alpha \cdot D_\beta, & -e_1 + e_2 &= B_1 \cdot D_\alpha \cdot D_\beta, & -e_2 + e_3 &= B_3 \cdot D_\alpha \cdot D_\beta, \\ -e_3 + e_4 &= B_4 \cdot D_\alpha \cdot D_\beta, & -e_4 + e_5 &= B_2 \cdot D_\alpha \cdot D_\beta, \end{aligned} \quad (\text{C.9})$$

in the hypersurface. D_α and D_β also satisfy the condition

$$S \cdot_{\mathcal{B}} D_\alpha \cdot_{\mathcal{B}} D_\beta = 1. \quad (\text{C.10})$$

One can always write down the negative simple roots from the intersection of the divisors due to the intersection (2.13). The intersection (C.9) in the hypersurface can be promoted to the intersection in the ambient space by further intersecting with the defining equation (C.8). When one restricts on the divisors D_i to consider the curves $\mathcal{C}_{-\alpha_i}$, the defining equation (C.8) is further reduced. Then, (C.9) become

$$\mathcal{C}_{e_1 - e_5} = E_0 \cap y^2E_3E_4 + a_1xyz - x^3E_1E_2^2E_3, \quad (\text{C.11})$$

$$\mathcal{C}_{-e_1 + e_2} = E_1 \cap y^2E_3E_4 + a_1xyz, \quad (\text{C.12})$$

$$\mathcal{C}_{-e_2 + e_3} = E_2 \cap y^2E_3E_4 + a_1xyz + a_{3,2}yz^3E_0^2E_1E_4, \quad (\text{C.13})$$

$$\begin{aligned} \mathcal{C}_{-e_3 + e_4} &= E_3 \cap (a_1xyz + a_{3,2}yz^3E_0^2E_1E_4 - a_{2,1}x^2z^2E_0E_1E_2 \\ & - a_{4,3}xz^4E_0^3E_1^2E_2E_4 - a_{6,5}z^6E_0^5E_1^3E_2E_4^2), \end{aligned} \quad (\text{C.14})$$

$$\mathcal{C}_{-e_4 + e_5} = E_4 \cap a_1xyz - x^3E_1E_2^2E_3 - a_{2,1}x^2z^2E_0E_1E_2. \quad (\text{C.15})$$

Here we omit the intersection $D_\alpha \cdot D_\beta$ in (C.9) since it is common for all the cases. If a divisor is written as E_1 for example, it should be understood as $E_1 = 0$.

Let us focus on the chain of the degeneration $A_4 \rightarrow D_5 \rightarrow E_6$ and $A_4 \rightarrow D_5 \rightarrow D_6$ for the phase I. Other chains and other phases can be understood in a similar manner. The D_5 singularity enhancement locus is characterized by $a_1 = 0$ ¹³. Along the locus $a_1 = 0$, two of

¹³To be precise, a_1 can be written as $a_1 = a_{1,0} + a_{1,1}w + \dots$. The **10** matter curve is obtained by imposing both $a_{1,0} = 0$ and $w = 0$. The latter condition is the restriction to S_b . From these two conditions, the **10** matter curve can be characterized just by $a_1 = 0$.

the curves of (C.11)–(C.15) further degenerate into smaller components. The curves along $a_1 = 0$ are

$$\mathcal{C}_{e_1-e_5} \rightarrow E_0 \cap y^2 E_4 - x^3 E_1 E_2^2, \quad (\text{C.16})$$

$$\mathcal{C}_{-e_1+e_2} \rightarrow E_1 \cap E_4, \quad (\text{C.17})$$

$$\mathcal{C}_{-e_2+e_3} \rightarrow E_2 \cap E_4, E_2 \cap y E_3 + a_{3,2} z^3 E_0^2 E_1, \quad (\text{C.18})$$

$$\begin{aligned} \mathcal{C}_{-e_2+e_3} \rightarrow E_3 \cap (a_{3,2} y z E_0 E_4 - a_{2,1} x^2 E_2 - a_{4,3} x z^2 E_0^2 E_1 E_2 E_4 \\ - a_{6,5} z^4 E_0^4 E_1^2 E_2 E_4^2), \end{aligned} \quad (\text{C.19})$$

$$\mathcal{C}_{-e_4+e_5} \rightarrow E_4 \cap E_1, E_4 \cap E_2, \quad (\text{C.20})$$

$$E_4 \cap -x E_2 E_3 - a_{2,1} z^2 E_0. \quad (\text{C.21})$$

In order to obtain this decomposition, we use the Stanley-Reisner ideal (4.22) for the phase I. Note that the curves corresponding to the weights $-e_2 + e_3$ and $-e_4 + e_5$ further decompose and one can identify them with the weights

$$E_2 \cap E_4 \rightarrow \mathcal{C}_{-e_2-e_4}, \quad (\text{C.22})$$

$$E_2 \cap y E_3 + a_{3,2} z^3 E_0^2 E_1 \rightarrow \mathcal{C}_{e_3+e_4}, \quad (\text{C.23})$$

$$E_4 \cap -x E_2 E_3 - a_{2,1} z^2 E_0 \rightarrow \mathcal{C}_{e_1+e_5}. \quad (\text{C.24})$$

This is consistent with the decomposition of (3.22) and (3.23). The intersection between the curves of (C.16)–(C.21) form the extended D_5 Dynkin diagram as depicted in Figure 2.

The E_6 enhancement point is characterized by $a_1 = 0$ and $a_{2,1} = 0$. The curves of (C.19) and (C.21) further degenerate as

$$\mathcal{C}_{-e_2+e_3} \rightarrow E_3 \cap E_4, \quad (\text{C.25})$$

$$E_3 \cap a_{3,2} y z - a_{4,3} x z^2 E_0 E_1 E_2 - a_{6,5} z^4 E_0^3 E_1^2 E_2 E_4, \quad (\text{C.26})$$

$$\mathcal{C}_{e_1+e_5} \rightarrow E_4 \cap E_2, E_4 \cap E_3. \quad (\text{C.27})$$

The other curves do not change. The identification of the weights is

$$E_3 \cap E_4 \rightarrow \mathcal{C}_{-e_3}, \quad (\text{C.28})$$

$$E_3 \cap (a_{3,2} y z - a_{4,3} x z^2 E_0 E_1 E_2 - a_{6,5} z^4 E_0^3 E_1^2 E_2 E_4) \rightarrow \mathcal{C}_{e_4}. \quad (\text{C.29})$$

$$(\text{C.30})$$

Therefore, we have six curves altogether

$$\mathcal{C}_{e_1-e_5}, \mathcal{C}_{-e_1+e_2}, \mathcal{C}_{-e_2-e_4}, \mathcal{C}_{e_3+e_4}, \mathcal{C}_{-e_3}, \mathcal{C}_{e_4} \quad (\text{C.31})$$

at the E_6 singularity enhancement points. They form the E_6 Dynkin diagram as depicted in Figure 2.

The D_6 enhancement point, on the other hand, is characterized by $a_1 = 0$ and $a_{3,2} = 0$. Then, (C.19) decomposes as

$$\mathcal{C}_{-e_2+e_3} \rightarrow E_3 \cap E_2, E_3 \cap \alpha_1 x + \beta_1 z^2 E_0^2 E_1 E_4, \quad (\text{C.32})$$

$$E_3 \cap \alpha_2 x + \beta_2 z^2 E_0^2 E_1 E_4, \quad (\text{C.33})$$

where $\alpha_{1,2}, \beta_{1,2}$ are constants which satisfy $\alpha_1\alpha_2 = -a_{2,1}$, $\alpha_1\beta_2 + \alpha_2\beta_1 = -a_{4,3}$, $\beta_1\beta_2 = -a_{6,5}$. The identification of the components in (C.33) with the weights is

$$E_3 \cap E_2 \rightarrow \mathcal{C}_{e_3+e_4}, \quad (\text{C.34})$$

$$E_3 \cap \alpha_1 x + \beta_1 z^2 E_0^2 E_1 E_4 \rightarrow \mathcal{C}_{-e_3}, \quad (\text{C.35})$$

$$E_3 \cap \alpha_2 x + \beta_2 z^2 E_0^2 E_1 E_4 \rightarrow \mathcal{C}_{-e'_3}. \quad (\text{C.36})$$

Hence we have seven curves altogether

$$\mathcal{C}_{e_1-e_5}, \mathcal{C}_{e_1+e_5}, \mathcal{C}_{-e_1+e_2}, \mathcal{C}_{-e_2-e_4}, \mathcal{C}_{e_3+e_4}, \mathcal{C}_{-e_3}, \mathcal{C}_{-e'_3} \quad (\text{C.37})$$

at the D_6 singularity enhancement points. They form the extended D_6 Dynkin diagram as depicted in Figure 2.

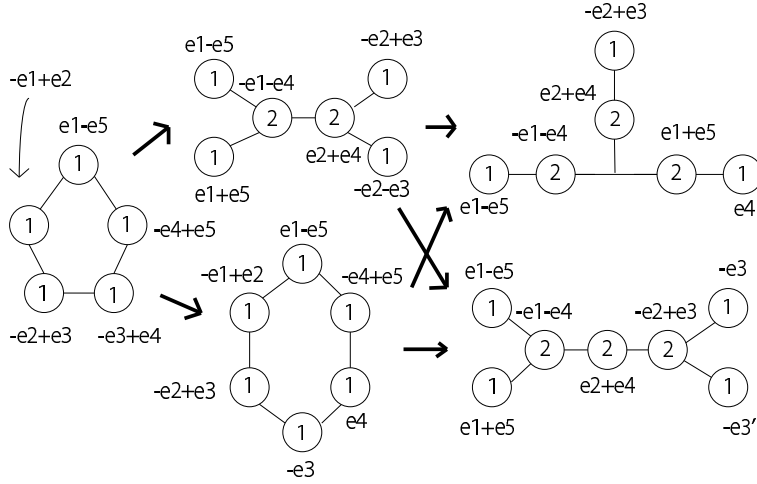


Figure 4: The chain of the Dynkin diagrams for the phase II. The number in the nodes denotes the multiplicity.

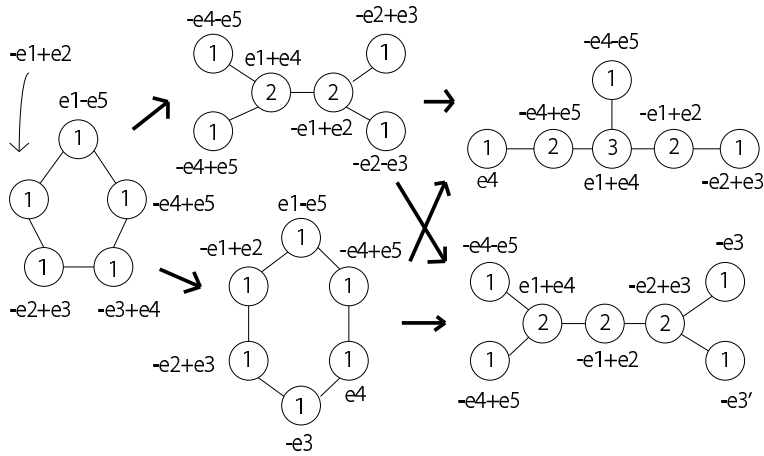


Figure 5: The chain of the Dynkin diagrams for the phase III. The number in the node denotes the multiplicity.

One can also do the same computation for the other phases. The chains of the Dynkin diagrams for the phase II are depicted in Figure 4 and the ones for the phase III are depicted in Figure 5. For the phase II, the E_6 enhancement points generate a $T_{3,3,3}^-$ diagram, not the E_6 Dynkin diagram. The two $\mathbf{10}$ weights and one $\overline{\mathbf{10}}$ weights form the junction-type intersection in the $T_{3,3,3}^-$ in Figure 4. The phase II is the only phase where three $\mathbf{10}$ or $\overline{\mathbf{10}}$ weights appear in the generators of the Mori cone. This may be a criterion to see whether the degeneration generates the E_6 Dynkin diagram or $T_{3,3,3}^-$ diagram from the generators of the relative Mori cone.

References

- [1] F. Denef, “Les Houches Lectures on Constructing String Vacua,” [arXiv:0803.1194 [hep-th]].
- [2] T. Weigand, “Lectures on F-theory compactifications and model building,” *Class. Quant. Grav.* **27** (2010) 214004. [arXiv:1009.3497 [hep-th]].
- [3] R. Donagi, M. Wijnholt, “Model Building with F-Theory,” [arXiv:0802.2969 [hep-th]].
- [4] C. Beasley, J. J. Heckman, C. Vafa, “GUTs and Exceptional Branes in F-theory - I,” *JHEP* **0901** (2009) 058. [arXiv:0802.3391 [hep-th]].
- [5] H. Hayashi, R. Tatar, Y. Toda, T. Watari, M. Yamazaki, “New Aspects of Heterotic–F Theory Duality,” *Nucl. Phys.* **B806** (2009) 224-299. [arXiv:0805.1057 [hep-th]].
- [6] R. Friedman, J. Morgan, E. Witten, “Vector bundles and F theory,” *Commun. Math. Phys.* **187** (1997) 679-743. [hep-th/9701162].
- [7] H. Hayashi, T. Kawano, Y. Tsuchiya, T. Watari, “More on Dimension-4 Proton Decay Problem in F-theory – Spectral Surface, Discriminant Locus and Monodromy,” *Nucl. Phys.* **B840** (2010) 304-348. [arXiv:1004.3870 [hep-th]].
- [8] T. W. Grimm, T. Weigand, “On Abelian Gauge Symmetries and Proton Decay in Global F-theory GUTs,” *Phys. Rev.* **D82** (2010) 086009. [arXiv:1006.0226 [hep-th]].
- [9] J. Marsano, N. Saulina, S. Schafer-Nameki, “Monodromies, Fluxes, and Compact Three-Generation F-theory GUTs,” *JHEP* **0908** (2009) 046. [arXiv:0906.4672 [hep-th]].
- [10] R. Blumenhagen, T. W. Grimm, B. Jurke, T. Weigand, “Global F-theory GUTs,” *Nucl. Phys.* **B829** (2010) 325-369. [arXiv:0908.1784 [hep-th]].
- [11] T. W. Grimm, S. Krause, T. Weigand, “F-Theory GUT Vacua on Compact Calabi-Yau Fourfolds,” *JHEP* **1007**, 037 (2010). [arXiv:0912.3524 [hep-th]].
- [12] J. Marsano, N. Saulina, S. Schafer-Nameki, “A Note on G-Fluxes for F-theory Model Building,” *JHEP* **1011** (2010) 088. [arXiv:1006.0483 [hep-th]];
J. Marsano, N. Saulina, S. Schafer-Nameki, “On G-flux, M5 instantons, and U(1)s in F-theory,” [arXiv:1107.1718 [hep-th]].
- [13] J. Marsano, S. Schafer-Nameki, “Yukawas, G-flux, and Spectral Covers from Resolved Calabi-Yau’s,” [arXiv:1108.1794 [hep-th]].
- [14] P. Candelas, A. Font, “Duality between the webs of heterotic and type II vacua,” *Nucl. Phys.* **B511** (1998) 295-325. [hep-th/9603170].

- [15] P. Candelas, E. Pevrvalov, G. Rajesh, “Toric geometry and enhanced gauge symmetry of F theory / heterotic vacua,” Nucl. Phys. **B507** (1997) 445-474. [hep-th/9704097].
- [16] M. Cvetic, I. Garcia-Etxebarria, J. Halverson, “Global F-theory Models: Instantons and Gauge Dynamics,” JHEP **1101** (2011) 073. [arXiv:1003.5337 [hep-th]].
- [17] C. -M. Chen, J. Knapp, M. Kreuzer, C. Mayrhofer, “Global SO(10) F-theory GUTs,” JHEP **1010** (2010) 057. [arXiv:1005.5735 [hep-th]];
J. Knapp, M. Kreuzer, C. Mayrhofer, N. -O. Walliser, “Toric Construction of Global F-Theory GUTs,” JHEP **1103** (2011) 138. [arXiv:1101.4908 [hep-th]].
- [18] S. Krause, C. Mayrhofer, T. Weigand, “G4 flux, chiral matter and singularity resolution in F-theory compactifications,” [arXiv:1109.3454 [hep-th]]
- [19] V. Braun, “Toric Elliptic Fibrations and F-Theory Compactifications,” [arXiv:1110.4883 [hep-th]].
- [20] M. Esole and S. T. Yau, “Small resolutions of SU(5)-models in F-theory,” arXiv:1107.0733 [hep-th].
- [21] T. W. Grimm, “The N=1 effective action of F-theory compactifications,” Nucl. Phys. **B845** (2011) 48-92. [arXiv:1008.4133 [hep-th]].
- [22] K. Dasgupta, G. Rajesh, S. Sethi, “M theory, orientifolds and G - flux,” JHEP **9908** (1999) 023. [hep-th/9908088]
- [23] M. Haack, J. Louis, “M theory compactified on Calabi-Yau fourfolds with background flux,” Phys. Lett. **B507** (2001) 296-304. [hep-th/0103068];
M. Haack, J. Louis, “Duality in heterotic vacua with four supercharges,” Nucl. Phys. **B575** (2000) 107-133. [hep-th/9912181].
- [24] A. P. Braun, A. Collinucci, R. Valandro, “G-flux in F-theory and algebraic cycles,” [arXiv:1107.5337 [hep-th]].
- [25] K. A. Intriligator, D. R. Morrison, N. Seiberg, “Five-dimensional supersymmetric gauge theories and degenerations of Calabi-Yau spaces,” Nucl. Phys. **B497** (1997) 56-100. [hep-th/9702198].
- [26] S. Katz, P. Mayr, C. Vafa, “Mirror symmetry and exact solution of 4-D N=2 gauge theories: 1.,” Adv. Theor. Math. Phys. **1** (1998) 53-114. [hep-th/9706110].
- [27] S. H. Katz, C. Vafa, “Matter from geometry,” Nucl. Phys. **B497** (1997) 146-154. [hep-th/9606086].
- [28] H. Hayashi, T. Kawano, R. Tatar, T. Watari, “Codimension-3 Singularities and Yukawa Couplings in F-theory,” Nucl. Phys. **B823** (2009) 47-115. [arXiv:0901.4941 [hep-th]].
- [29] R. Tatar, Y. Tsuchiya, T. Watari, “Right-handed Neutrinos in F-theory Compactifications,” Nucl. Phys. **B823** (2009) 1-46. [arXiv:0905.2289 [hep-th]].
- [30] F. Bonetti and T. W. Grimm, “Six-dimensional (1,0) effective action of F-theory via M-theory on Calabi-Yau threefolds,” arXiv:1112.1082 [hep-th].
- [31] E. Witten, “Phases of N=2 theories in two-dimensions,” Nucl. Phys. **B403** (1993) 159-222. [hep-th/9301042].
- [32] E. Witten, “On flux quantization in M theory and the effective action,” J. Geom. Phys. **22** (1997) 1-13. [hep-th/9609122].

- [33] A. Collinucci, R. Savelli, “On Flux Quantization in F-Theory,” [arXiv:1011.6388 [hep-th]].
- [34] T. W. Grimm, T. -W. Ha, A. Klemm, D. Klevers, “Computing Brane and Flux Superpotentials in F-theory Compactifications,” *JHEP* **1004** (2010) 015. [arXiv:0909.2025 [hep-th]].
- [35] T. W. Grimm, M. Kerstan, E. Palti, T. Weigand, “Massive Abelian Gauge Symmetries and Fluxes in F-theory,” [arXiv:1107.3842 [hep-th]].
- [36] T. W. Grimm, R. Savelli, “Gravitational Instantons and Fluxes from M/F-theory on Calabi-Yau fourfolds,” [arXiv:1109.3191 [hep-th]].
- [37] J. Wess, J. Bagger, “Supersymmetry and supergravity,” Princeton, USA: Univ. Pr. (1992) 259 p.
- [38] O. Aharony, A. Hanany, K. A. Intriligator, N. Seiberg, M. J. Strassler, “Aspects of N=2 supersymmetric gauge theories in three-dimensions,” *Nucl. Phys.* **B499** (1997) 67-99. [hep-th/9703110].
- [39] P. Berglund, S. H. Katz, A. Klemm, “Mirror symmetry and the moduli space for generic hypersurfaces in toric varieties,” *Nucl. Phys.* **B456** (1995) 153-204. [hep-th/9506091].
- [40] P. Berglund, S. H. Katz, A. Klemm, P. Mayr, “New Higgs transitions between dual N=2 string models,” *Nucl. Phys.* **B483** (1997) 209-228. [hep-th/9605154].
- [41] V. Braun, P. Candelas, X. De La Ossa, A. Grassi, “Toric Calabi-Yau fourfolds duality between N=1 theories and divisors that contribute to the superpotential,” [hep-th/0001208].
- [42] J. Knapp, M. Kreuzer, “Toric Methods in F-theory Model Building,” *Adv. High Energy Phys.* **2011** . [arXiv:1103.3358 [hep-th]].
- [43] G. Curio, “Chiral matter and transitions in heterotic string models,” *Phys. Lett.* **B435** (1998) 39-48. [hep-th/9803224].
- [44] D. -E. Diaconescu, G. Ionesi, “Spectral covers, charged matter and bundle cohomology,” *JHEP* **9812** (1998) 001. [hep-th/9811129].
- [45] G. Curio, R. Y. Donagi, “Moduli in N=1 heterotic / F theory duality,” *Nucl. Phys.* **B518** (1998) 603-631. [hep-th/9801057].
- [46] W. Taylor, “TASI Lectures on Supergravity and String Vacua in Various Dimensions,” [arXiv:1104.2051 [hep-th]].
- [47] V. Kumar, W. Taylor, “String Universality in Six Dimensions,” [arXiv:0906.0987 [hep-th]]; V. Kumar, D. R. Morrison, W. Taylor, “Global aspects of the space of 6D N = 1 supergravities,” *JHEP* **1011** (2010) 118. [arXiv:1008.1062 [hep-th]].
- [48] D. R. Morrison, W. Taylor, “Matter and singularities,” [arXiv:1106.3563 [hep-th]].
- [49] D. S. Park, W. Taylor, “Constraints on 6D Supergravity Theories with Abelian Gauge Symmetry,” [arXiv:1110.5916 [hep-th]].
- [50] V. Sadov, “Generalized Green-Schwarz mechanism in F theory,” *Phys. Lett.* **B388** (1996) 45-50. [hep-th/9606008].
- [51] M. B. Green, J. H. Schwarz, “Anomaly Cancellation in Supersymmetric D=10 Gauge Theory and Superstring Theory,” *Phys. Lett.* **B149** (1984) 117-122.
- [52] A. Sagnotti, “A Note on the Green-Schwarz mechanism in open string theories,” *Phys. Lett.* **B294** (1992) 196-203. [hep-th/9210127].